NASA TECHNICAL NOTE

NASA TN D-6282

e. 1

NASA TN D-6282

MEASUREMENT OF ELECTRON DENSITY
OF A NEGATIVE-GLOW PLASMA WITH
AN E-BAND FABRY-PEROT INTERFEROMETER

by Bruce M. Kendall

Langley Research Center
Hampton, Va. 23365

1. Report No. NASA TN D-6282	2. Government Accession No.	3. Recipient's Catalog No.
4. Title and Subtitle MEASUREMENT OF ELECTRON DENSITY OF A NEGATIVE-GLOW PLASMA WITH AN E-BAND FABRY-PEROT INTERFEROMETER		5. Report Date June 1971
		6. Performing Organization Code
7. Author(s) Bruce M. Kendall		8. Performing Organization Report No. L-7656
9. Performing Organization Name and Address NASA Langley Research Center Hampton, Va. 23365		10. Work Unit No. 125-21-14-01
		11. Contract or Grant No.
12. Sponsoring Agency Name and Address National Aeronautics and Space Administration Washington, D.C. 20546		13. Type of Report and Period Covered Technical Note
		14. Sponsoring Agency Code

15. Supplementary Notes The material presented herein was offered as a thesis entitled "Investigation of Plasma Electron Density at E-Band using a Fabry-Perot Interferometer" in partial satisfaction of the requirements for the degree of Master of Science, The George Washington University, Washington, D.C., June 1970.

16. Abstract

Electron-density measurements of a negative-glow plasma were made at E-band (60 to 90 GHz) with a Fabry-Perot interferometer. These measurements demonstrated the validity of the technique of using a flat-plate Fabry-Perot interferometer, which provided a closer approximation to plane-wave theory than the spherical-mirror resonators previously used for electron-density measurement. In addition, this technique provides for the analysis of inhomogeneous plasma with a parabolic distribution of electron density, which has not been reported previously.

Measurements made at separate frequencies of 60.3, 76.6, and 89.1 GHz demonstrated to within a factor of 2 the frequency independence and repeatability of the measurement technique. Also, the results of the Fabry-Perot interferometer measurements agreed well with those obtained independently for the same plasma with an X-band and K-band microwave interferometer. A comparison between the derived equations of electron density for the assumed homogeneous plasma slab and the inhomogeneous plasma with parabolic distribution show that the slab approximation is valid for such an electron density profile.

17. Key Words (Suggested by Author(s)) Plasma physics Fabry-Perot interferometer Plasma electron density Perturbation theory	18. Distribution Statement Unclassified — Unlimited		
19. Security Classif. (of this report) Unclassified	20. Security Classif. (of this page) Unclassified	21. No. of Pages 41	22. Price* $3.00

MEASUREMENT OF ELECTRON DENSITY OF A NEGATIVE-GLOW PLASMA

WITH AN E-BAND FABRY-PEROT INTERFEROMETER*

By Bruce M. Kendall
Langley Research Center

SUMMARY

Electron-density measurements of a negative-glow plasma were made at E-band (60 to 90 GHz) with a Fabry-Perot interferometer. These measurements demonstrated the validity of the technique of using a flat-plate Fabry-Perot interferometer, which provided a closer approximation to plane-wave theory than the spherical-mirror resonators previously used for electron-density measurement. In addition, this technique provides for the analysis of inhomogeneous plasma with a parabolic distribution of electron density, which has not been reported previously.

Measurements made at separate frequencies of 60.3, 76.6, and 89.1 GHz demonstrated to within a factor of 2 the frequency independence and repeatability of the measurement technique. Also, the results of the Fabry-Perot interferometer measurements agreed well with those obtained independently for the same plasma with an X-band and K-band microwave interferometer. A comparison between the derived equations of electron density for the assumed homogeneous plasma slab and the inhomogeneous plasma with parabolic distribution show that the slab approximation is valid for such an electron density profile.

INTRODUCTION

The properties of plasmas have long been of considerable interest to engineers and physicists engaged in reentry communications research. In order to study the effects on radio-frequency communications of a plasma or ionized gas layer which surrounds a spacecraft upon reentry into the earth's atmosphere, several laboratory-generated plasmas have been used at the Langley Research Center of the National Aeronautics and Space Administration. One such plasma was generated with helium gas by means of a rectangular laminated cathode (ref. 1).

One of the most important plasma properties is the electron density or number of free electrons per unit volume. The purpose of this study is to investigate a laboratory microwave measurement technique for obtaining this parameter. In this technique, the

---

plasma to be studied is inserted between the reflector plates of a microwave Fabry-Perot cavity operating under resonance conditions. The plasma causes a perturbation within the cavity which results in a shift in resonance frequency.

In the millimeter and submillimeter wavelength regions, conventional microwave-cavity resonators become increasingly difficult to build with reasonable tolerances and relatively high quality factors, since their dimensions must be comparable to the operating wavelength. The advantage of the flat-plate Fabry-Perot interferometer shown in figure 1 (from ref. 2) is that in the millimeter region its physical dimensions are large compared with the operating wavelength, and the maintenance of a high quality factor is easier. A high quality factor produces a sharp cavity response, which is necessary in this study for accurate measurement of the resonance frequency. A discussion of the fundamental operation of the Fabry-Perot interferometer is found in appendix A.

The Fabry-Perot interferometer has been previously used at the Langley Research Center to measure dielectric constants and losses of dielectric material at V-band (ref. 2) and E-band (ref. 3). The use of a Fabry-Perot interferometer to measure plasma properties of a laboratory-generated plasma has been reported elsewhere (refs. 4 to 7).

The first measurements of electron density with a Fabry-Perot interferometer were made by Primich and Hayami (ref. 7). They performed a uniform plane-wave analysis for a plane lossless dielectric slab in a plane parallel-plate Fabry-Perot resonator and argued that this analysis also applied for a spherical mirror resonator. Although they constructed a focused 70-GHz Fabry-Perot resonator, they made no plasma measurements with it but used it to make dielectric-constant measurements on a dry gas. Lonngren, Mink, and Beyer (ref. 4) utilized perturbation theory to derive diagnostic relations for a Fabry-Perot resonator containing a homogeneous, isotropic, cold plasma slab. The derived equations expressed the theoretical behavior of the complex resonant frequency of the resonator as a function of the complex dielectric constant of the plasma slab. The real part of the dielectric constant was thus shown to cause a resonance shift. The derived equations are also significant in that they indicate the possibility of allowing for electron density gradients. Actual measurement of the electron density of a cylindrical neon plasma column was accomplished by Chaffin and Beyer (refs. 5 and 6), using a 35-GHz confocal Fabry-Perot resonator with spherical mirrors. However, their theory was dependent on assuming the column of plasma to be closely approximated by a plasma slab.

The E-band Fabry-Perot interferometer constructed at the Langley Research Center to measure the electron density of a laminated-cathode discharge plasma used flat-plate mirrors which allowed a closer approximation in the use of uniform plane-wave theory. Measurements with Langmuir probes had shown that this plasma had a parabolic distribution of electron density along the line of measurement, which was

2

transverse to the axis of the plasma tube (ref. 1). Therefore, extending the previous work, equations were derived for the determination of electron density which allowed for an electron density profile along the direction of propagation. Also, for the purpose of comparison, equations were derived for the idealized case of the homogeneous plasma slab.

The measurements of electron density made with the E-band Fabry-Perot interferometer were also compared with measurements made with a conventional X-band and K-band microwave interferometer.

SYMBOLS

a, b	distances between centers of coupling holes along orthogonal axes
c	velocity of light, 2.998×10^{10} cm/sec
d	distance between reflector plates
E	electric field intensity of perturbed cavity
E_O	electric field intensity of unperturbed cavity
E_t	electric field intensity of cavity transverse to direction of propagation
f_O	resonant frequency of unperturbed cavity
Δf	half-power bandwidth of cavity
H	magnetic field intensity of perturbed cavity
H_O	magnetic field intensity of unperturbed cavity
k_O	wave number of unperturbed cavity, ω_O/c
n_{av}	average value of electron density for parabolic distribution, $\frac{2}{3} n_{max}$
n_e	electron density
n_{max}	peak value of electron density for parabolic distribution

Q	quality factor of perturbed cavity
Q_O	quality factor of unperturbed cavity
r	radius of coupling holes
τ_O	transmission coefficient
V	total volume of cavity
ΔV	volume of material inserted in cavity
x,y,z	Cartesian coordinates
Y_O	characteristic admittance of free space
ΔZ	thickness of plasma slab
β	phase constant
ϵ	permittivity of plasma inserted in cavity
ϵ_O	permittivity of unperturbed cavity
$\Delta \epsilon$	change in permittivity due to cavity perturbation
μ_O	permeability of unperturbed cavity
$\Delta \mu$	change in permeability due to cavity perturbation
ν	plasma collision frequency
ρ_O	reflection coefficient
ω	natural resonant frequency of perturbed cavity
ω_O	natural resonant frequency of unperturbed cavity
ω_p	plasma frequency

Ω complex resonant frequency of perturbed cavity

Ω_0 complex resonant frequency of unperturbed cavity

A bar over a symbol denotes a vector.

An asterisk denotes complex conjugate.

RESONANT-CAVITY PERTURBATIONAL THEORY

The change in the resonant frequency of a cavity may be discussed in terms of a material perturbation within the cavity (ref. 8). Let $\overline{E}_0$, $\overline{H}_0$, and Ω_0 represent the fields and complex resonant frequency of the unperturbed cavity, and $\overline{E}$, $\overline{H}$, and Ω the corresponding quantities of the perturbed cavity. If ϵ_0 and μ_0 are the permittivity and permeability, respectively, of the unperturbed cavity, and $\Delta\epsilon$ and $\Delta\mu$ are their corresponding changes due to the perturbation of the cavity, it can be shown (ref. 8) that for a lossless medium,

$$\frac{\Omega - \Omega_0}{\Omega} = - \frac{\iiint_{\Delta V}\left(\Delta\epsilon\overline{E} \cdot \overrightarrow{E}_0^* + \Delta\mu\overline{H} \cdot \overrightarrow{H}_0^*\right)dv}{\iiint_V\left(\epsilon_0\overline{E} \cdot \overrightarrow{E}_0^* + \mu_0\overline{H} \cdot \overrightarrow{H}_0^*\right)dv} \tag{1}$$

where ΔV is the volume of the material inserted in the cavity and V is the total volume of the cavity.

However, as $\Delta\epsilon$ and $\Delta\mu$ approach zero, $\overline{E}$ and $\overline{H}$ can be approximated by $\overline{E}_0$ and $\overline{H}_0$ to obtain

$$\frac{\Omega - \Omega_0}{\Omega} \approx - \frac{\iiint_{\Delta V}\left(\Delta\epsilon\left|\overline{E}_0\right|^2 + \Delta\mu\left|\overline{H}_0\right|^2\right)dv}{\iiint_V\left(\epsilon_0\left|\overline{E}_0\right|^2 + \mu_0\left|\overline{H}_0\right|^2\right)dv} \tag{2}$$

Since finite losses are present, caused by diffraction and reflection from the end plates of a Fabry-Perot resonator, the resonant frequencies are expressible in complex form (ref. 4) as

$$\Omega_0 = \omega_0\left(1 + \frac{j}{2Q_0}\right) \tag{3}$$

$$\Omega = \omega\left(1 + \frac{j}{2Q}\right) \tag{4}$$

5

where ω_O and ω are the natural resonant frequencies for the unperturbed and perturbed condition, respectively, and Q_O and Q are their corresponding quality factors. Equations (3) and (4) can be combined to yield

$$\frac{\Omega - \Omega_O}{\Omega} \approx \frac{\omega - \omega_O}{\omega} + \frac{j}{2} \frac{Q_O - Q}{Q_O Q} \tag{5}$$

for high cavity Q values. If the perturbation material introduced into the cavity is a plasma of volume ΔV and permittivity ϵ, not only are the Ω's complex, but the μ's and ϵ's too. Also, at resonance the magnetic and electric energies are equal.

If it is assumed that $\Delta\mu = 0$ for a plasma with no applied static magnetic field, equation (2) can now be written as

$$\frac{\Omega - \Omega_O}{\Omega} = - \frac{\iiint_{\Delta V} \Delta\epsilon \left|\overline{E}_O\right|^2 dv}{2 \iiint_V \epsilon_O \left|\overline{E}_O\right|^2 dv} \tag{6}$$

The dielectric constant of a cold, lossy, isotropic plasma without an applied static magnetic field can be simplified from a tensor quantity to the following expression (from ref. 6):

$$\epsilon = \epsilon_O \left(1 - \frac{\omega_p^2}{\omega^2 - j\omega\nu} \right) \tag{7}$$

where ω_p is the plasma frequency and ν the collision frequency. Thus

$$\Delta\epsilon = \epsilon - \epsilon_O = -\epsilon_O \left(\frac{\omega_p^2/\omega^2}{1 + \frac{\nu^2}{\omega^2}} + j \frac{\omega_p^2\nu/\omega^3}{1 + \frac{\nu^2}{\omega^2}} \right) \tag{8}$$

Substituting equation (8) into equation (6) gives

$$\frac{\Omega - \Omega_O}{\Omega} = \frac{\iiint_{\Delta V} \left(\frac{\omega_p^2/\omega^2}{1 + \frac{\nu^2}{\omega^2}} + j \frac{\omega_p^2\nu/\omega^3}{1 + \frac{\nu^2}{\omega^2}} \right) \left|\overline{E}_O\right|^2 dv}{2 \iiint_V \left|\overline{E}_O\right|^2 dv} \tag{9}$$

If $\nu \ll \omega$, which was true for the plasma investigated ($\nu/\omega < 0.01$), equation (9) reduces to

6

$$\frac{\Omega - \Omega_0}{\Omega} = \frac{\iiint_{\Delta V}\left[\left(\omega_p{}^2/\omega^2\right) + j\left(\omega_p{}^2\nu/\omega^3\right)\right]\left|\overline{E}_0\right|^2 dv}{2\iiint_V \left|\overline{E}_0\right|^2 dv} \tag{10}$$

Equating the real and imaginary parts of equation (10) to those of equation (5) results in

$$\frac{\omega - \omega_0}{\omega} = \frac{\iiint_{\Delta V}\left(\omega_p{}^2/\omega^2\right)\left|\overline{E}_0\right|^2 dv}{2\iiint_V \left|\overline{E}_0\right|^2 dv} \tag{11}$$

$$\frac{Q_0 - Q}{Q_0 Q} = \frac{\iiint_{\Delta V}\left(\omega_p{}^2\nu/\omega^3\right)\left|\overline{E}_0\right|^2 dv}{\iiint_V \left|\overline{E}_0\right|^2 dv} \tag{12}$$

Equations (11) and (12) are similar to those obtained in reference 5, but ω is used in place of ω_0 in the denominator of the left-hand side of equation (11).

Variations of electron density and collision frequency are allowed in the transverse and longitudinal directions by equations (11) and (12). Therefore, both equations could be integrated for assumed spatial distributions. An expression for the plasma frequency is given by reference 9:

$$\omega_p{}^2 = \left(5.64 \times 10^4\right)^2 n_e \tag{13}$$

where n_e is the electron density per cubic centimeter. The field solutions in the Fabry-Perot resonator with transverse electromagnetic (TEM) standing waves can be expressed (ref. 5) as

$$\overline{E}_0 = \overline{E}_t \cos\left(k_0 z\right) \tag{14}$$

$$\overline{H}_0 = jY_0\overline{E}_t \sin\left(k_0 z\right) \tag{15}$$

with z measured from the center of the cavity as shown in figure 2. Since the reflecting plates have a reflection coefficient approximately equal to 1 (see ref. 2), a good approximation is obtained by letting E_0 equal zero at $z = \pm\frac{d}{2}$:

$$\cos\left(k_0 \frac{d}{2}\right) = 0 \tag{16a}$$

or

$$k_0 d = l\pi \qquad (l = 1, 3, 5, \ldots) \tag{16b}$$

The transverse electric field for the flat-plate resonator has very small values at the edges of the plates. (See refs. 10 and 11.) When equations (13) and (14) are substituted into equation (11) integration is necessary only in the z-direction, since integrations in the transverse directions in the numerator would cancel with those in the denominator (assuming that the field distribution along the transverse direction is the same in the plasma and in free space and allowing for electron density variation in the z-direction only). Performing this operation yields

$$2(\omega - \omega_0)\omega = \left(5.64 \times 10^4\right)^2 \frac{\int_{-\Delta Z/2}^{\Delta Z/2} n_e \cos^2(k_0 z)\,dz}{\int_{-d/2}^{d/2} \cos^2(k_0 z)\,dz} \tag{17}$$

In analyzing the Fabry-Perot resonator with finite plates, the assumption is made that the field between the reflectors is a TEM standing wave. (See ref. 12.) This can exist only for infinite flat plates. Finite reflector plates must have an amplitude variation along the transverse axes so that the amplitude falls to a negligible value at the edges of the reflector plates (ref. 12). Since there are many field distributions that would meet this requirement, there are many possible modes of oscillation for a Fabry-Perot resonator with finite reflectors. (See refs. 10 and 11.) However, these modes are all approximately TEM waves, as the transverse dimensions are large in terms of wavelength.

Homogeneous Density Distribution

For the homogeneous density distribution, a plasma slab of uniform electron density (n_e = Constant) and of infinite cross section is assumed to be inserted between the plates of the resonator as shown in figure 2, where d is the distance between the end plates and ΔZ the slab thickness. For this case equation (17) can be written as

$$2(\omega - \omega_0)\omega = \left(5.64 \times 10^4\right)^2 n_e \frac{\int_{-\Delta Z/2}^{\Delta Z/2} \cos^2(k_0 z)\,dz}{\int_{-d/2}^{d/2} \cos^2(k_0 z)\,dz} \tag{18}$$

which, solved for n_e, may be rewritten as

$$n_e = \frac{2\omega(\omega - \omega_0)}{\left(5.64 \times 10^4\right)^2} \frac{\int_{-d/2}^{d/2} \cos^2(k_0 z)\,dz}{\int_{-\Delta Z/2}^{\Delta Z/2} \cos^2(k_0 z)\,dz} \tag{19}$$

When the integrations are performed, equation (19) reduces to

$$n_e = \frac{2\omega(\omega - \omega_0)}{\left(5.64 \times 10^4\right)^2} \frac{d}{\Delta Z + \frac{\sin\left(k_0 \Delta Z\right)}{k_0}} \tag{20}$$

which can be rewritten as

$$n_e = \frac{2\omega(\omega - \omega_0)}{\left(5.64 \times 10^4\right)^2} \frac{1}{P} \tag{21}$$

where

$$P = \frac{\Delta Z}{d} + \frac{\sin\left(k_0 \Delta Z\right)}{k_0 d}$$

Equation (21) expresses the electron density of a homogeneous plasma slab in terms of parameters which can be measured during an investigation. Therefore, for a given d and ΔZ, the electron density may be determined by measuring the resonant frequency of the cavity before and during the perturbation caused by the plasma.

<div align="center">Inhomogeneous Density Distribution</div>

For the case of inhomogeneous plasma, the electron density is assumed to have a parabolic distribution. The equation for the electron density may be expressed as

$$n_e = n_{max}\left[-\left(\frac{2}{\Delta Z}\right)^2 z^2 + 1\right] \tag{22}$$

where n_{max} is the peak value of electron density as shown in figure 3. If equation (22) for n_e is now substituted into the general expression given in equation (17), the result is

$$2(\omega - \omega_0)\omega = \left(5.64 \times 10^4\right)^2 n_{max} \frac{\int_{-\Delta Z/2}^{\Delta Z/2}\left[-\left(\frac{2}{\Delta Z}\right)^2 z^2 + 1\right]\cos^2\left(k_0 z\right)dz}{\int_{-d/2}^{d/2} \cos^2\left(k_0 z\right)dz} \tag{23}$$

which may be rewritten for n_{max} as

$$n_{max} = \frac{2\omega(\omega - \omega_0)}{\left(5.64 \times 10^4\right)^2} \frac{\int_{-d/2}^{d/2} \cos^2\left(k_0 z\right)dz}{\int_{-\Delta Z/2}^{\Delta Z/2}\left[-\left(\frac{2}{\Delta Z}\right)^2 z^2 + 1\right]\cos^2\left(k_0 z\right)dz} \tag{24}$$

Equation (24) may be expanded to

$$n_{max} = \frac{2\omega(\omega - \omega_0)}{(5.64 \times 10^4)^2} \frac{\int_{-d/2}^{d/2} \cos^2(k_0 z)dz}{-\frac{4}{(\Delta Z)^2}\int_{-\Delta Z/2}^{\Delta Z/2} z^2\cos^2(k_0 z)dz + \int_{-\Delta Z/2}^{\Delta Z/2} \cos^2(k_0 z)dz} \tag{25}$$

Performing the respective integrations yields

$$\int_{-d/2}^{d/2} \cos^2(k_0 z) = \frac{d}{2} \tag{26a}$$

$$\int_{-\Delta Z/2}^{\Delta Z/2} \cos^2(k_0 z)dz = \frac{\Delta Z}{2} + \frac{\sin(k_0 \Delta Z)}{2k_0} \tag{26b}$$

$$-\frac{4}{(\Delta Z)^2}\int_{-\Delta Z/2}^{\Delta Z/2} z^2\cos^2(k_0 z)dz = -\frac{\Delta Z}{6} - \left[\frac{1}{2k_0} - \frac{1}{k_0^3(\Delta Z)^2}\right]\sin(k_0 \Delta Z) - \frac{\cos(k_0 \Delta Z)}{k_0^2 \Delta Z} \tag{26c}$$

When equations (26a), (26b), and (26c) are substituted into equation (25), the result is

$$n_{max} = \frac{\omega(\omega - \omega_0)}{(5.64 \times 10^4)^2} \frac{d}{\frac{\Delta Z}{3} + \frac{\sin(k_0 \Delta Z)}{k_0^3(\Delta Z)^2} - \frac{\cos(k_0 \Delta Z)}{k_0^2 \Delta Z}} \tag{27}$$

which may be rewritten as

$$n_{max} = \frac{2\omega(\omega - \omega_0)}{(5.64 \times 10^4)^2} \frac{1}{P'} \tag{28}$$

where

$$P' = \frac{2}{d}\left[\frac{\Delta Z}{3} + \frac{\sin(k_0 \Delta Z)}{k_0^3(\Delta Z)^2} - \frac{\cos(k_0 \Delta Z)}{k_0^2 \Delta Z}\right]$$

Equation (28) represents the maximum or peak value of electron density for a plasma with parabolic distribution. The average value of electron density is given by

$$n_{av} = \frac{2}{3} n_{max} \tag{29}$$

If equation (29) is divided by equation (20), with equation (27) substituted for n_{max}, the result is

$$\frac{n_{av}}{n_e} = \frac{1 + \dfrac{\sin(k_0\Delta Z)}{k_0\Delta Z}}{1 + 3\dfrac{\sin(k_0\Delta Z)}{(k_0\Delta Z)^3} - 3\dfrac{\cos(k_0\Delta Z)}{(k_0\Delta Z)^2}} \tag{30}$$

Inspection of equation (30) reveals that the sine and cosine terms are negligible and therefore the ratio of n_{av} to n_e is approximately 1. The different dependence of n_{av} and n_e on k_0 and ΔZ through the sine and cosine terms prevents the ratio from being exactly 1. However, the approximation itself shows that a plasma with a parabolic distribution of electron density can be defined by an equivalent uniform plasma slab of constant electron density.

SYSTEM DESCRIPTION

E-Band Fabry-Perot Interferometer

Photographs of the system used to measure the electron density of a plasma generated by a rectangular brush cathode are shown in figure 4. A block diagram of the E-band Fabry-Perot interferometer measurement system is shown in figure 5.

The interferometer framework consisted mainly of two flat aluminum plates which were 266.7 by 177.8 by 9.525 mm with a 134.94-mm-diameter hole in the center, and four steel support rods 304.8 mm long and 9.525 mm in diameter. The support rods were attached to the main frame of the plasma tube and protruded through a hole in each corner of the plates as shown in figures 6(a) and (b). Setscrews allowed the plates to be positioned parallel to each other on the support rods and on each side of the rectangular glass plasma container shown in figure 7. An E-band horn was attached to an aluminum mounting bracket on each plate. A photograph of the horn and mounting bracket assembled on one of the flat plates is shown in figure 8. The horns were conical with 50.8-mm-diameter collimating lens.

The interferometer reflector plates were thin (0.0254-mm) perforated membranes about 127 mm in diameter. The membranes were constructed of nickel and coated with a thin film of gold to increase the conductivity of the surface. A photograph of the reflector membrane mounted on one of the flat plates of the interferometer is shown in figure 9. Figure 10 (from ref. 3) shows the hole pattern of the membranes, with dimensions of $a = b = 2.54$ mm and $r = 0.508$ mm. This design represented a compromise to obtain a relatively high Q for sharpness of the cavity response curve and good transmission for a detectable signal.

The resonant frequency of the interferometer cavity was measured by means of the system shown in figure 5. The frequency of the E-band backward-wave oscillator (BWO)

was varied, and the response of the Fabry-Perot resonant cavity was displayed on the oscilloscope as shown in figure 11(a). A harmonic of the phase-locked X-band klystron output was mixed with part of the E-band BWO output. The frequency of the X-band klystron was varied until a zero beat was obtained from the harmonic mixer. The zero beat was simultaneously displayed on the dual-beam oscilloscope with the cavity response curve, as shown in figure 11(b), and was used as a variable-frequency marker. When the zero beat was alined with the cavity center (resonant) frequency at the peak of the response curve, the corresponding frequency was indicated by the X-band frequency counter; this frequency, when multiplied by the proper harmonic number, gave the cavity resonant frequency at E-band.

This same technique was used to determine the half-power bandwidth points from the cavity response curve in order to compute the Q_0 of the cavity from the formula

$$Q_0 = \frac{f_0}{\Delta f} \tag{31}$$

where f_0 is the resonant frequency of the cavity and Δf is the half-power bandwidth of the cavity. The measured Q_0 of the E-band Fabry-Perot interferometer cavity was approximately 6700.

Brush-Cathode Plasma Tube

In this experiment a negative-glow plasma (refs. 1 and 13) was generated with helium by a rectangular laminated cathode about 63.5 by 190.5 mm. The plasma was confined to a rectangular volume by a glass container, shown in figure 7, which was 203.2 by 69.85 by 457.2 mm. A 152.4-mm-diameter hole was cut in the center of the top and bottom plates and covered with 0.0254-mm Mylar to allow the propagation of E-band frequency through the glass tube structure within the Fabry-Perot resonator cavity. The entire structure was housed in a cylindrical glass vacuum container which was 457.2 mm in diameter and 1219.2 mm long, with vacuum-sealed metal end plates, as shown in figures 4(a) and (b).

EXPERIMENTAL TECHNIQUE AND RESULTS

By means of the system shown in figure 5, measurements of electron density were made on a plasma generated with a rectangular brush cathode and helium gas. The resonant frequency of the cavity, with and without the plasma, was measured by using the cavity response curve and variable-frequency marker as discussed in a preceding section.

Electron Density Measurement

Electron density measurements were made for several values of tube current at each of four separate tube pressures, 0.125, 0.210, 0.410, and 0.680 torr (1 torr = 133.3 N/m^2).

These measurements were made within a 5 to 10 minute warmup period of the plasma, at three discrete frequencies (60.3, 76.6, and 89.1 GHz) in the E-band frequency range.

The known values of plate separation (d = 9.525 cm) and plasma thickness (ΔZ = 6.096 cm) were used to compute the values of electron density for the assumed homogeneous plasma from equation (21). The results are shown in figure 12, where electron density is plotted as a function of plasma tube current for the three measurement frequencies and four tube pressures.

An analysis of the accuracy of the reported values for electron density (see appendix B) has shown maximum errors of +23 percent and -16 percent for the assumed homogeneous plasma and +20 percent and -18 percent for the inhomogeneous plasma. Therefore, the reported values of electron density were accurate to within approximately 20 percent or better.

<div align="center">Comparison of Fabry-Perot and Microwave Interferometer Measurements</div>

Measurements of electron density of the plasma investigated with the E-band Fabry-Perot interferometer were made independently with an X-band and K-band microwave interferometer. The results are presented in figure 13 for a tube pressure of 0.410 torr and in figure 14 for a tube pressure of 0.680 torr. These figures show values of peak electron density as measured by the Fabry-Perot interferometer compared with the values as obtained from the X-band and K-band microwave interferometer measurements for the same tube conditions. The diagonal line represents perfect agreement. It should be noted that the data points are consistently above the line of perfect agreement by about a constant factor. Also, the bars which show the error range for the X-band and K-band microwave interferometer measurements more than overlap the line of perfect agreement for the lower values of electron densities.

<div align="center">CONCLUDING REMARKS</div>

The results of this investigation have demonstrated the validity of the technique of using a flat-plate Fabry-Perot interferometer for the measurement of plasma electron density. In addition, this investigation has treated, for the first time with measured data, the case of the inhomogeneous plasma with a parabolic distribution of electron density in one direction. A comparison between the derived equations of electron density for the assumed homogeneous plasma slab and the inhomogeneous plasma with parabolic distribution show that the slab approximation is valid for such an electron density profile. The technique used to derive the equations of this investigation could be used in the analysis of other plasmas that have a particular electron density distribution in one direction and could also be expanded to handle distributions in the transverse directions.

Measurements made at separate frequencies of 60.3, 76.6, and 89.1 GHz demonstrated to within a factor of 2 the frequency independence and repeatability of the measurement technique. Thermal instability of the plasma being investigated prevented repeated measurements of electron density at a given measurement frequency and plasma-tube pressure.

The results of the E-band Fabry-Perot interferometer measurements agreed well with those obtained independently for the same plasma with an X-band and K-band microwave interferometer. This lends a factor of confidence to the values obtained for the electron density of the plasma investigated. The constant deviation from the line of perfect agreement was due in part to the inability to repeat identical plasma conditions.

Langley Research Center,
    National Aeronautics and Space Administration,
        Hampton, Va., May 25, 1971.

APPENDIX A

FABRY-PEROT INTERFEROMETER

The fundamental operation of the Fabry-Perot interferometer can be found in several sources (e.g., refs. 3, 12, 14, 15, 16, and 17). The resonator quality factor Q is a function of diffraction and reflection losses and of plate separation. It may be defined (ref. 14) as

$$Q = \omega \frac{\text{Energy stored}}{\text{Energy lost per second}} \tag{32}$$

and given by

$$Q = \frac{2\pi d}{\alpha \lambda} \tag{33}$$

where

d   distance between reflector plates

λ operating wavelength

α fractional power loss per bounce from reflector plate (sum of diffraction and reflection losses)

Since the Fabry-Perot interferometer is characterized by the absence of sidewalls, sidewall losses generally associated with cavities of lower microwave frequencies have been eliminated. However, as a result of the finite size of the reflector plates and imperfections in flatness, diffraction losses are introduced, but they may be controlled by appropriate plate separation and plate size. Misalinement of the plates from true parallelism increases diffraction losses and reduces Q. The reflection losses are caused by the ohmic absorption in the reflector plates and the coupling or transmission through the small coupling holes.

Since diffraction and reflection losses are both functions of reflector plate separation, at some point the combination of the two will be such that a maximum value of Q is achieved. For a given reflector size, Q increases with plate separation d until the diffraction losses become comparable with reflection losses, at which point a maximum Q is obtained. Further increase in plate separation then decreases Q by increasing the diffraction losses.

The Fabry-Perot resonant cavity can be considered as an interference light filter. (See ref. 18.) If the reflector plate surfaces were perfect conductors, resonance would occur and the electric field intensity at the boundary would be zero when the separation

15

between the plates was an integral number of half-wavelengths. For that spacing the metallic plate surfaces would not absorb energy from the electromagnetic wave. In practice, however, such a surface is not attainable, but surfaces with reflection coefficients close to 1 can be obtained. Since an ideal electric field node cannot be obtained, the wave absorption in the light filter is due to ohmic losses caused by induction of currents in the metallic surfaces.

Transmission through the light filter is calculated by considering multiple reflection of plane waves in the resonant cavity, shown in figure A1 (from ref. 3). If the
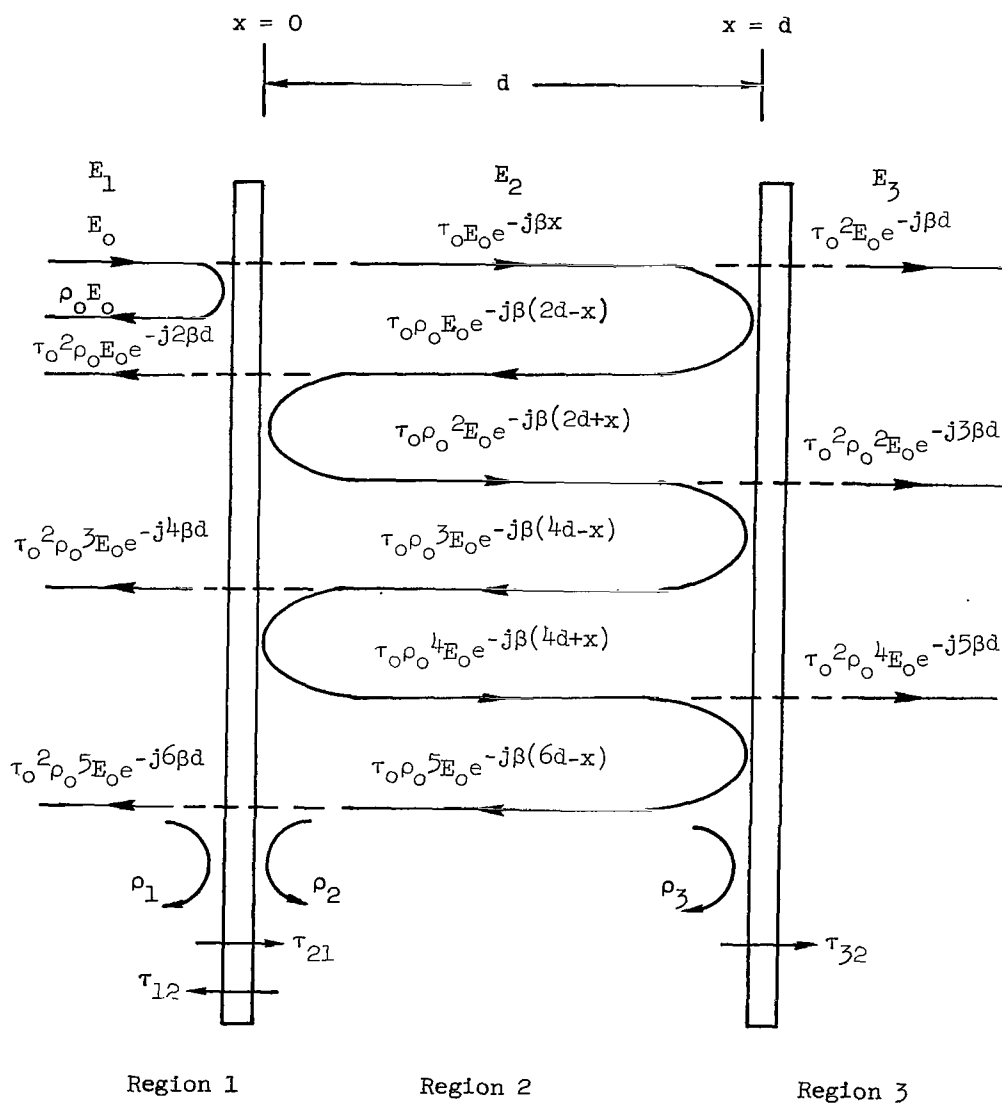
Figure A1.- Flat-plate resonant cavity.

transmission coefficients are assumed to be $\tau_{12} = \tau_{21} = \tau_{32} = \tau_0$ and the reflection coefficients are assumed to be $\rho_1 = \rho_2 = \rho_3 = \rho_0$, the fields in the various regions can then be calculated. In region 1 the reflected field E_1 is

$$E_1 = \rho_0 E_0 + \tau_0^2 \rho_0 E_0 e^{-j2\beta d} + \tau_0^2 \rho_0^3 E_0 e^{-j4\beta d} + \tau_0^2 \rho_0^5 E_0 e^{-j6\beta d} + \ldots$$

$$= \rho_0 E_0 \left[1 + \tau_0^2 e^{-j2\beta d} \left(1 + \rho_0^2 e^{-j2\beta d} + \rho_0^4 e^{-j4\beta d} + \ldots \right) \right]$$

$$= \rho_0 E_0 \left(1 + \tau_0^2 e^{-j2\beta d} \frac{1}{1 - \rho_0^2 e^{-j2\beta d}} \right)$$

Therefore,

$$\frac{E_1}{E_0} = \frac{\rho_0 \left[1 + \left(\tau_0^2 - \rho_0^2 \right) e^{-j2\beta d} \right]}{1 - \rho_0^2 e^{-j2\beta d}} \tag{34}$$

The ratio $\left| \dfrac{E_1}{E_0} \right|$ represents the total reflection coefficient of the resonant cavity. The field in region 2 is found to be

$$E_2 = \tau_0 E_0 e^{-j\beta x} + \tau_0 \rho_0 E_0 e^{-j\beta(2d-x)} + \tau_0 \rho_0^2 E_0 e^{-j\beta(2d+x)}$$

$$+ \tau_0 \rho_0^3 E_0 e^{-j\beta(4d-x)} + \tau_0 \rho_0^4 E_0 e^{-j\beta(4d+x)} + \ldots$$

$$= \tau_0 E_0 e^{-j\beta x} \left[1 + \rho_0 e^{-j2\beta(d-x)} + \rho_0^2 e^{-j2\beta d} + \rho_0^3 e^{-j2\beta(2d-x)} + \ldots \right]$$

$$= \tau_0 E_0 e^{-j\beta x} \left[1 + \rho_0 e^{-j2\beta(d-x)} \right] \left(1 + \rho_0^2 e^{-j2\beta d} + \rho_0^4 e^{-j4\beta d} + \ldots \right)$$

$$\frac{E_2}{E_0} = \frac{\tau_0 e^{-j\beta x} \left[1 + \rho_0 e^{-j2\beta(d-x)} \right]}{1 - \rho_0^2 e^{-j2\beta d}} \tag{35}$$

The field in region 3 is

$$E_3 = \tau_0^2 E_0 e^{-j\beta d} + \tau_0^2 \rho_0^2 E_0 e^{-j3\beta d} + \tau_0^2 \rho_0^4 E_0 e^{-j5\beta d} + \ldots$$

$$= \tau_0^2 E_0 e^{-j\beta d} \left(1 + \rho_0^2 e^{-j2\beta d} + \rho_0^4 e^{-j4\beta d} + \ldots \right)$$

$$\frac{E_3}{E_o} = \frac{\tau_o^2 e^{-j\beta d}}{1 - \rho_o^2 e^{-j2\beta d}} \tag{36}$$

The ratio $\left|\frac{E_3}{E_o}\right|$ represents the transmission coefficient of the entire cavity.

Optimum spacing for maximum transmission can be found by inspection of the ratio $\left|\frac{E_3}{E_o}\right|$:

$$\left|\frac{E_3}{E_o}\right| = \frac{\tau_o^2}{\left|1 - \rho_o^2 e^{-j2\beta d}\right|} \tag{37}$$

Maximum transmission occurs when

$$\beta d = \frac{n\pi}{2} \qquad (n = 2, 4, 6, \ldots) \tag{38}$$

or

$$d = \frac{\lambda}{2}, \ \lambda, \ \frac{3\lambda}{2}, \ldots \tag{39}$$

Minimum transmission occurs when

$$\beta d = \frac{n\pi}{2} \qquad (n = 1, 3, 5, \ldots) \tag{40}$$

or

$$d = \frac{\lambda}{4}, \ \frac{3\lambda}{4}, \ \frac{5\lambda}{4}, \ldots \tag{41}$$

The magnetic fields in the three regions, which can be found by the same procedure as was used in obtaining the electric fields, are given by

$$H_1 = -\frac{\rho_o Y_o E_o \left(1 + e^{-j2\beta d}\right)}{1 - \rho_o^2 e^{-j2\beta d}} \tag{42}$$

$$H_2 = \frac{\tau_o Y_o E_o e^{-j\beta x}\left[1 - \rho_o e^{-j2\beta(d-x)}\right]}{1 - \rho_o^2 e^{-j2\beta d}} \tag{43}$$

$$H_3 = \frac{\tau_o^2 Y_o E_o e^{-j\beta d}}{1 - \rho_o^2 e^{-j2\beta d}} \tag{44}$$

APPENDIX B

ERROR ANALYSIS

To determine the degree of confidence that can be placed in the reported values for the electron density, an error analysis was performed. As seen from equations (20) and (27), the calculated values for electron density were influenced by the accuracy of the measured variables ω, ω_0, d, and ΔZ. The plasma thickness ΔZ and reflector plate separation d can be measured to within ± 2.54 mm. The values of ω and ω_0 were primarily influenced by two factors: the accuracy of the X-band frequency counter and the alinement of the zero beat which was used as a frequency marker. The manufacturer's specified accuracy of the counter was 1 part in 10^6, or ± 1 kHz. It was possible to aline the zero-beat frequency marker with the center of the Fabry-Perot resonant cavity response curve on the oscilloscope to an accuracy within the maximum width of the zero beat shown in figure 11(b), which at X-band was ± 0.3 MHz.

To determine how much error could be associated with the calculated values of electron density, a maximum-error or worst-case analysis was performed on the basis of the specified accuracies for the measured variables ω_0, ω, ΔZ, and d. Inspection of equation (20), for the homogeneous plasma, indicates that for maximum error in the calculation of n_e in the positive sense or above the true value, ω should be increased and ω_0 decreased by their respective accuracies to obtain a maximum value for $(\omega - \omega_0)$ in the numerator. Also, the value of d in the numerator should be increased by its accuracy. The value of ΔZ in the denominator should be decreased as its value is much greater than the absolute value in the term $\dfrac{\sin(k_0 \Delta Z)}{k_0}$. Reversing this procedure (decreasing ω and d and increasing ω_0 and ΔZ) will result in values of n_e with maximum error in the negative sense, or below the true value. A similar analysis can be performed for the inhomogeneous plasma on the basis of equation (27). The percent error in the calculated values can then be determined from

$$\text{Percent error} = \left| \frac{\text{Adjusted value} - \text{Reported value}}{\text{Reported value}} \right| \times 100 \qquad (45)$$

where the adjusted value is the maximum or minimum value obtained from the preceding error analysis.

Performance of the above error analysis resulted in values for maximum error of +23 percent and -16 percent for the assumed homogeneous plasma and +20 percent and -18 percent for the inhomogeneous plasma. Therefore, the accuracy of the reported values of electron density was within approximately 20 percent or better.

REFERENCES

1. Roberts, Albert S., Jr.; and Grantham, William L.: Evaluation of an Abnormal-Glow Discharge for Use as a Laboratory Plasma Source. NASA TN D-6136, 1971.

2. Balanis, Constantine A.: Investigation of a Proposed Technique for Measurements of Dielectric Constants and Losses at V-band Using the Fabry-Perot Principle. M. E.E. Thesis, Univ. of Virginia, 1966.

3. Balanis, Constantine A.: Measurements of Dielectric Constants and Loss Tangents at E-Band Using a Fabry-Perot Interferometer. NASA TN D-5583, 1969.

4. Lonngren, K. E.; Mink, J. W.; and Beyer, J. B.: On the Focused Fabry-Perot Resonator in Plasma Diagnostics. IEEE Trans. Microwave Theory Tech., vol. MTT-12, no. 5, Sept. 1964, pp. 548-549.

5. Chaffin, Roger James: Application of the Microwave Fabry-Perot Resonator to Plasma Diagnostics. Ph. D. Thesis, Univ. of Wisconsin, 1967.

6. Chaffin, Roger J.; and Beyer, James B.: Plasma Diagnostics With a Microwave Fabry-Perot Resonator. IEEE Trans. Microwave Theory Tech., vol. MTT-16, no. 1, Jan. 1968, pp. 37-45.

7. Primich, R. I.; and Hayami, R. A.: The Application of the Focussed Fabry-Perot Resonator to Plasma Diagnostics. IEEE Trans. Microwave Theory Tech., vol. MTT-12, no. 1, Jan. 1964, pp. 33-42.

8. Harrington, Roger F.: Time-Harmonic Electromagnetic Fields. McGraw-Hill Book Co., Inc., 1961, pp. 321-323.

9. Holt, E. H.; and Haskell, R. E.: Foundations of Plasma Dynamics. Macmillan Co., c.1965, p. 256.

10. Fox, A. G.; and Li, Tingye: Resonant Modes in a Maser Interferometer. Bell System Tech. J., vol. 40, no. 2, Mar. 1961, pp. 453-488.

11. Fox, A. G.; and Li, T.: Resonant Modes in an Optical Maser. Proc. IRE, vol. 48, no. 11, Nov. 1960, pp. 1904-1905.

12. Collin, Robert E.: Foundations for Microwave Engineering. McGraw-Hill Book Co., Inc., 1966, pp. 337-344.

13. Persson, Karl-Birger: Brush Cathode Plasma – A Well-Behaved Plasma. J. Appl. Phys., vol. 36, no. 10, Oct. 1965, pp. 3086-3094.

14. Boyd, G. D.; and Gordon, J. P.: Confocal Multimode Resonator for Millimeter Through Optical Wavelength Masers. Bell System Tech. J., vol. 40, no. 2, Mar. 1961, pp. 489-508.

15. Culshaw, William: High Resolution Millimeter Wave Fabry-Perot Interferometer. IRE, Trans. Microwave Theory Tech., vol. MTT-8, no. 2, Mar. 1960, pp. 182-189.

16. Boyd, G. D.; and Kogelnik, H.: Generalized Confocal Resonator Theory. Bell System Tech. J., vol. 41, no. 4, July 1962, pp. 1347-1369.

17. Zimmerer, R. W.; Anderson, M. V.; Strine, G. L.; and Beers, Y.: Millimeter Wavelength Resonant Structures. IEEE Trans. Microwave Theory Tech., vol. MTT-11, no. 2, Mar. 1963, pp. 142-149.

18. Brekhovskikh, Leonid M. (David Lieberman, trans.): Waves in Layered Media. Academic Press Inc., c.1960.
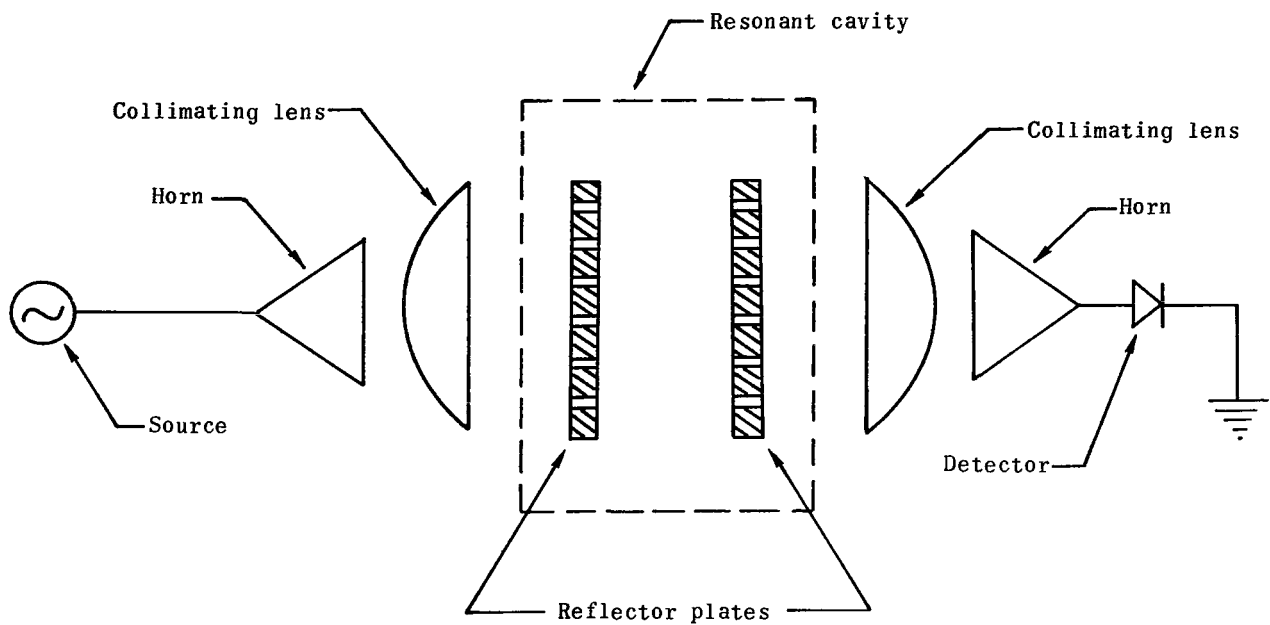
Figure 1.- Flat-plate Fabry-Perot interferometer.
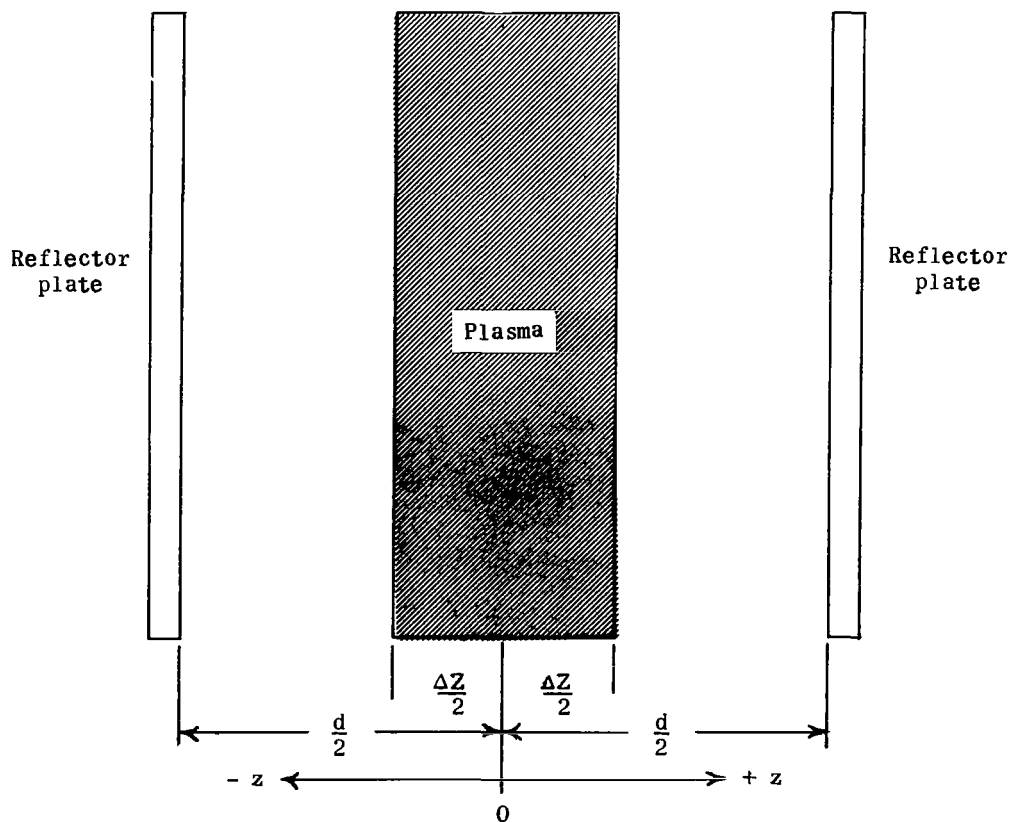
Figure 2.- Arrangement of reflector plates and plasma.
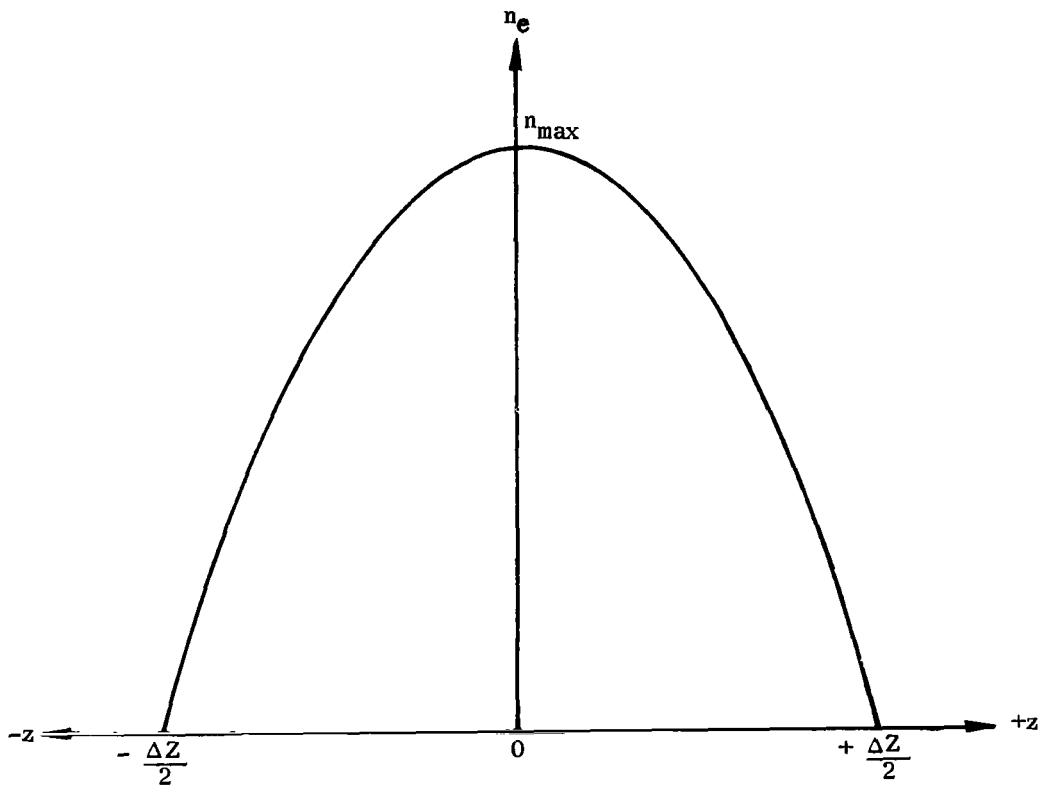
Figure 3.- Parabolic distribution of electron density for
an inhomogeneous plasma.
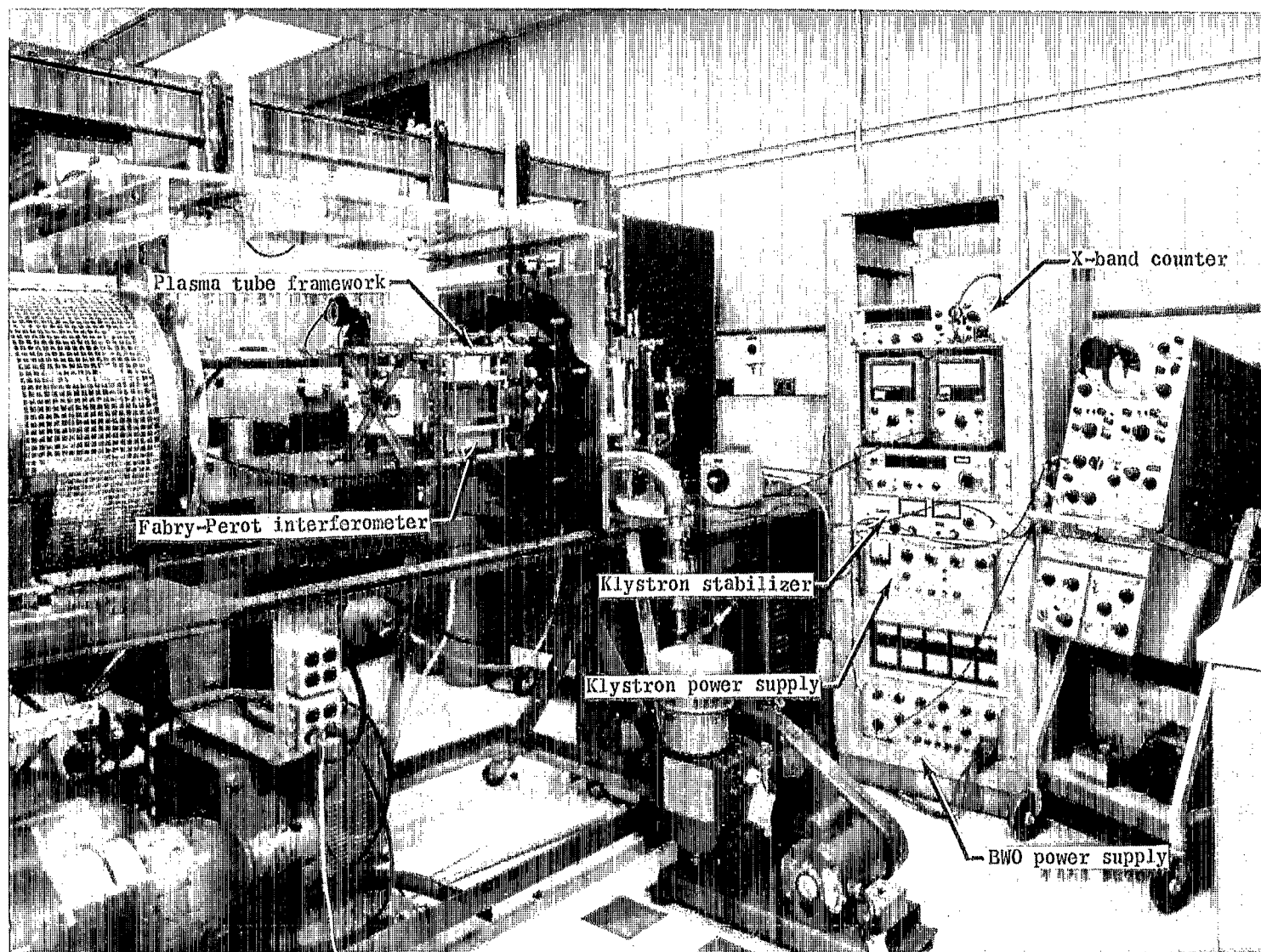
L-69-7547.1

(a) Plasma tube open.

Figure 4.- System used for the measurement of plasma electron density at E-band.

Glass vacuum container
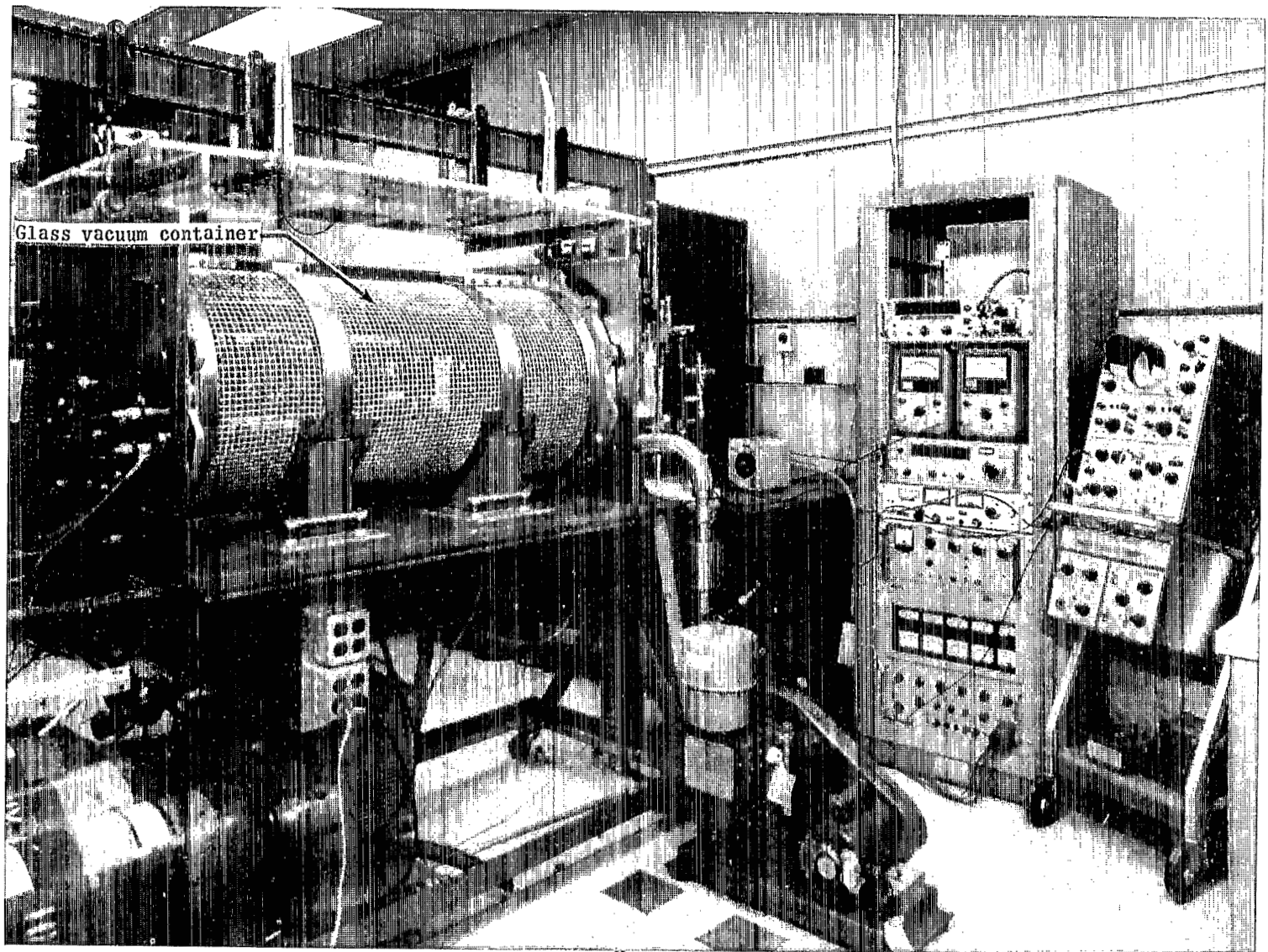
L-69-7553.1

(b) Plasma tube closed.

Figure 4.- Continued.
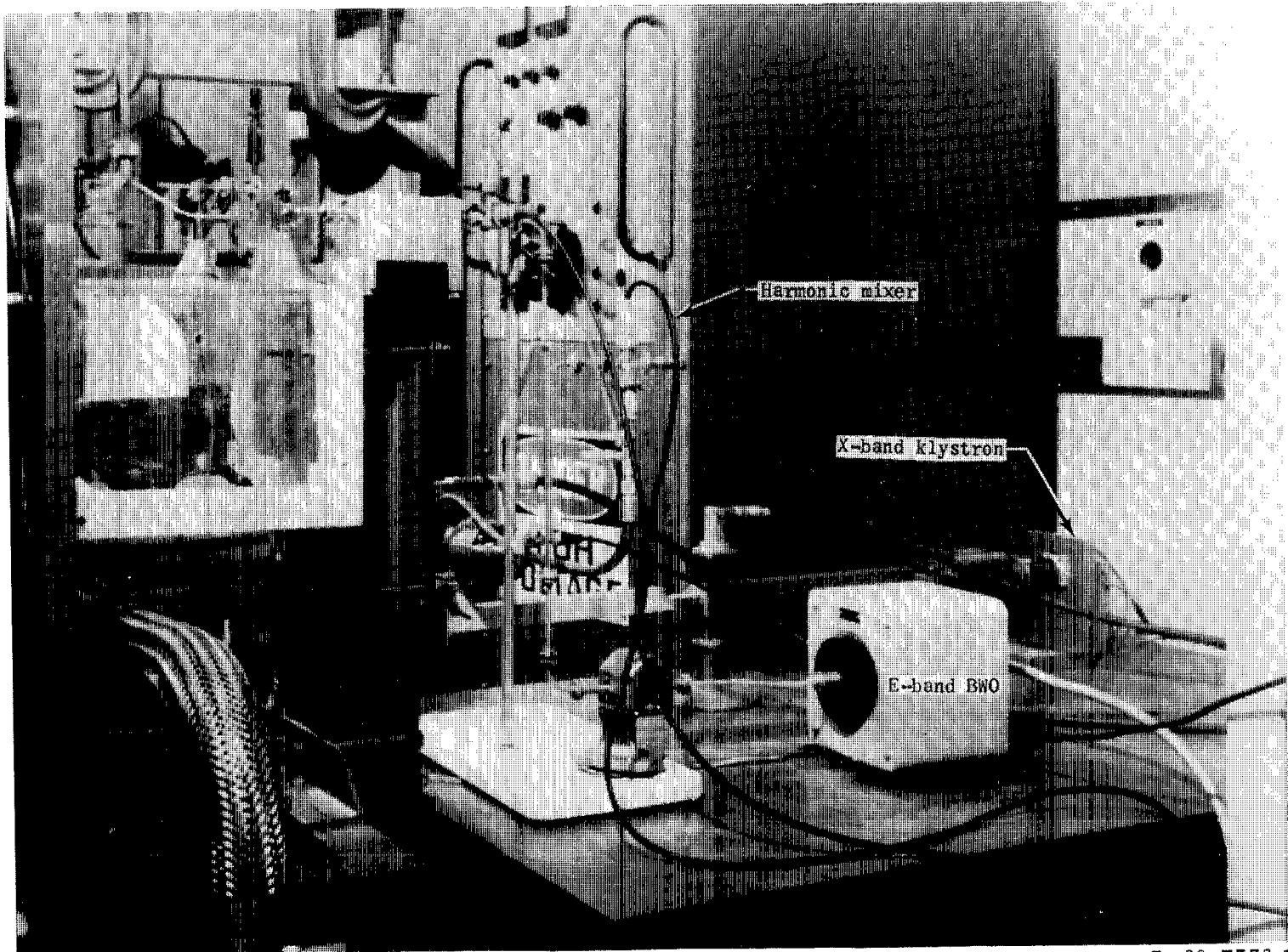
L-69-7550.1

(c) X-band and E-band waveguide systems.

Figure 4.- Concluded.
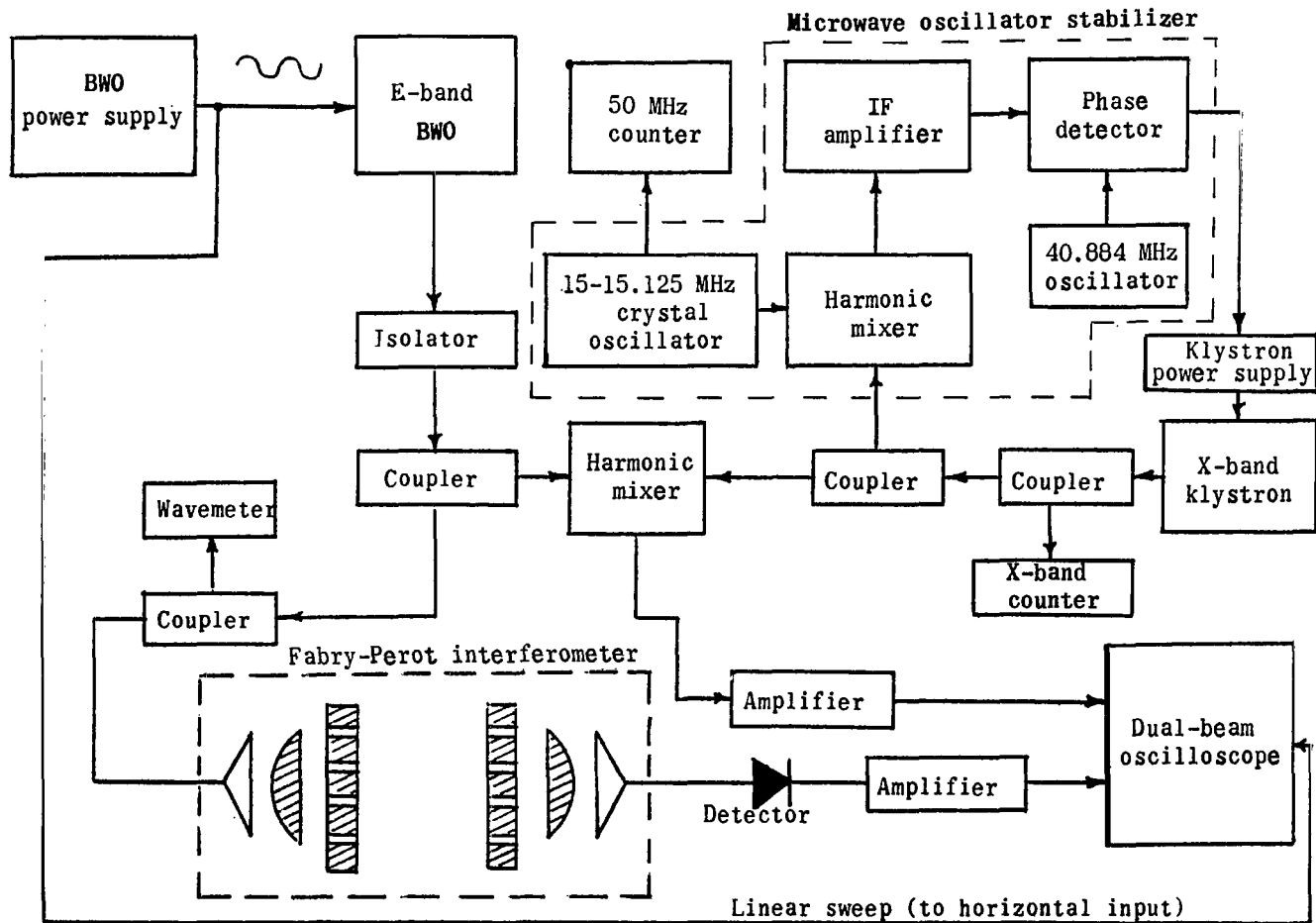
Figure 5.- Block diagram of system for measurement of plasma electron density at E-band.
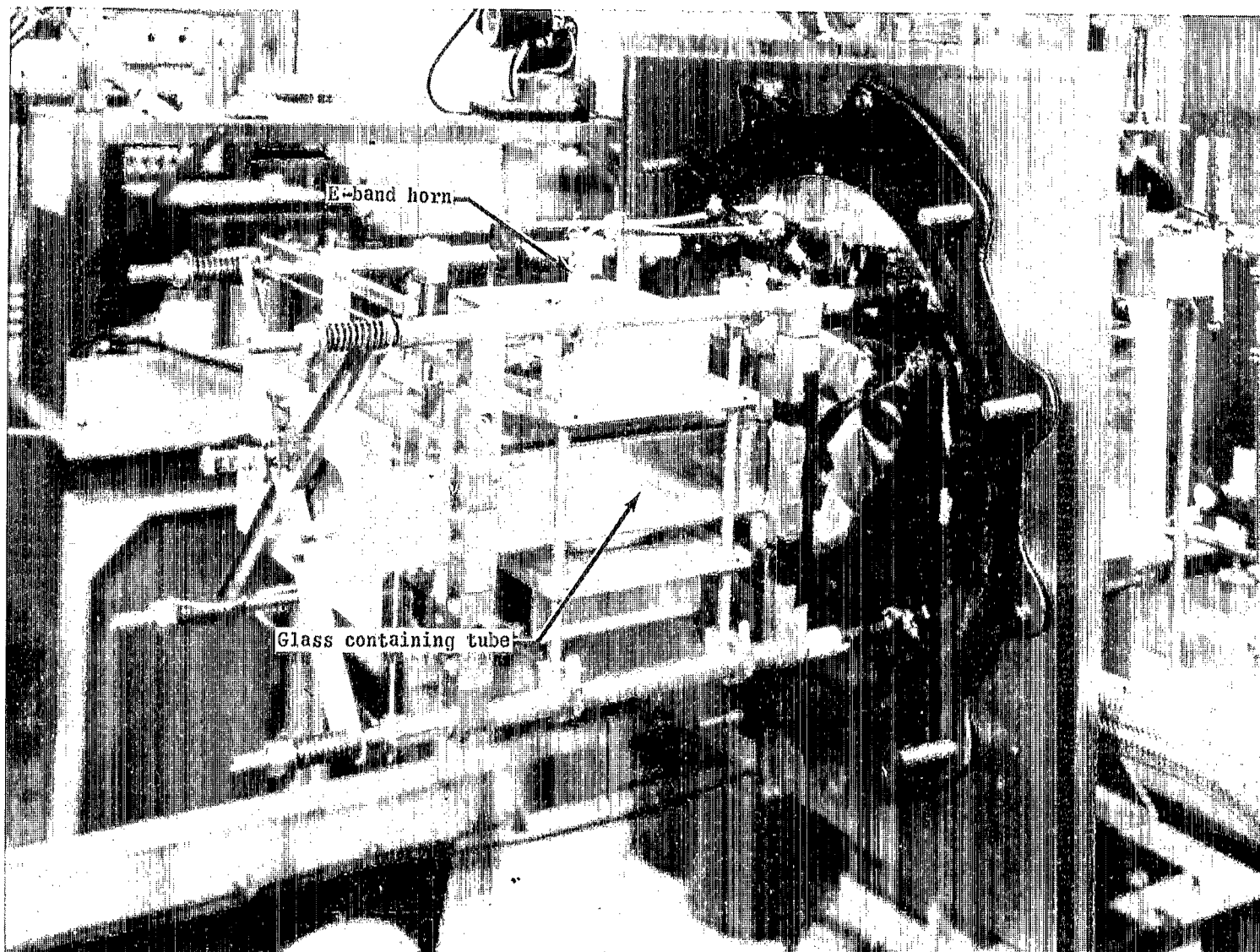
L-69-7551.1

(a) With rectangular containing tube.

Figure 6.- E-band Fabry-Perot interferometer.
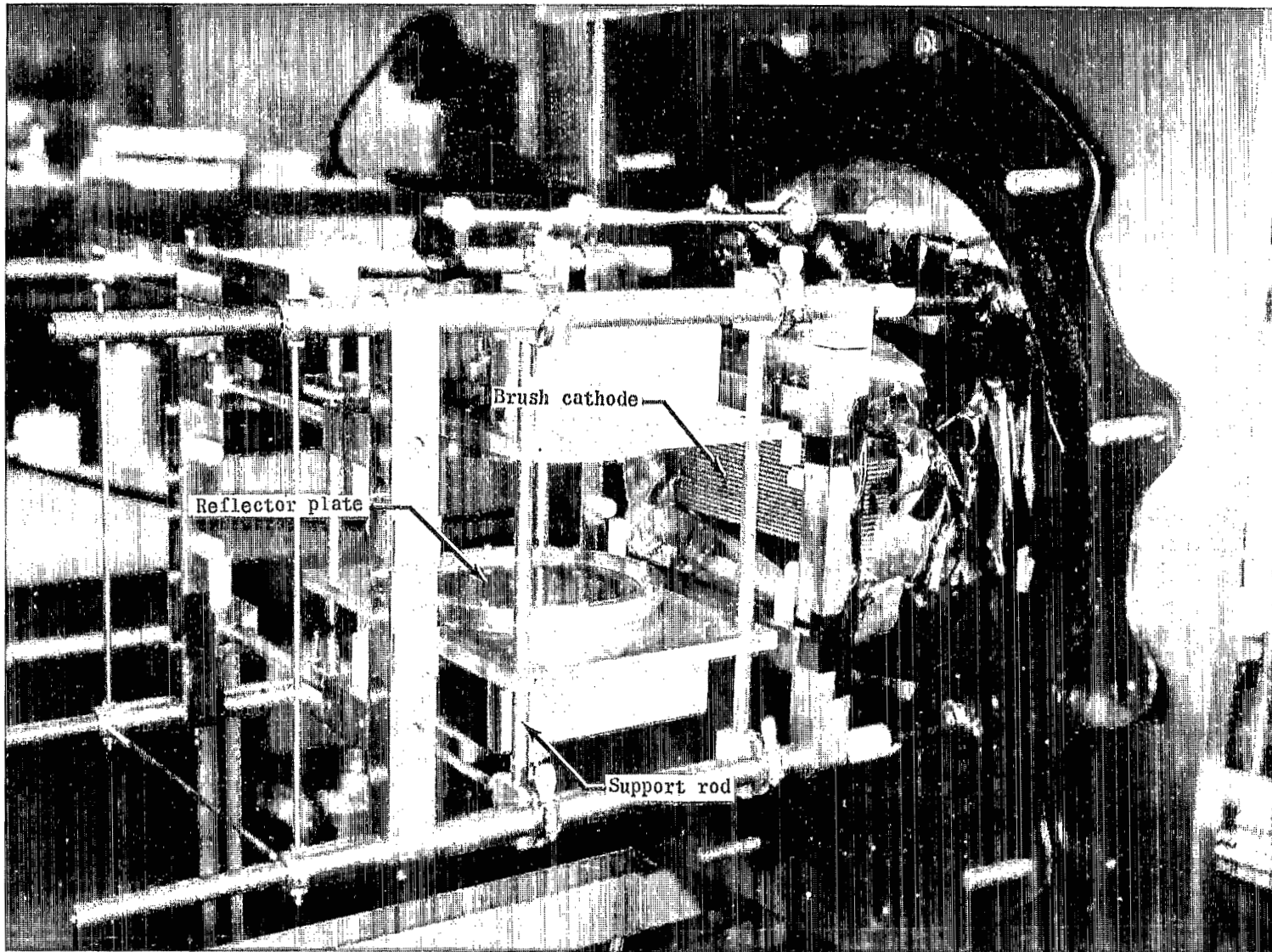
L-69-7554.1

(b) Without rectangular containing tube.

Figure 6.- Concluded.
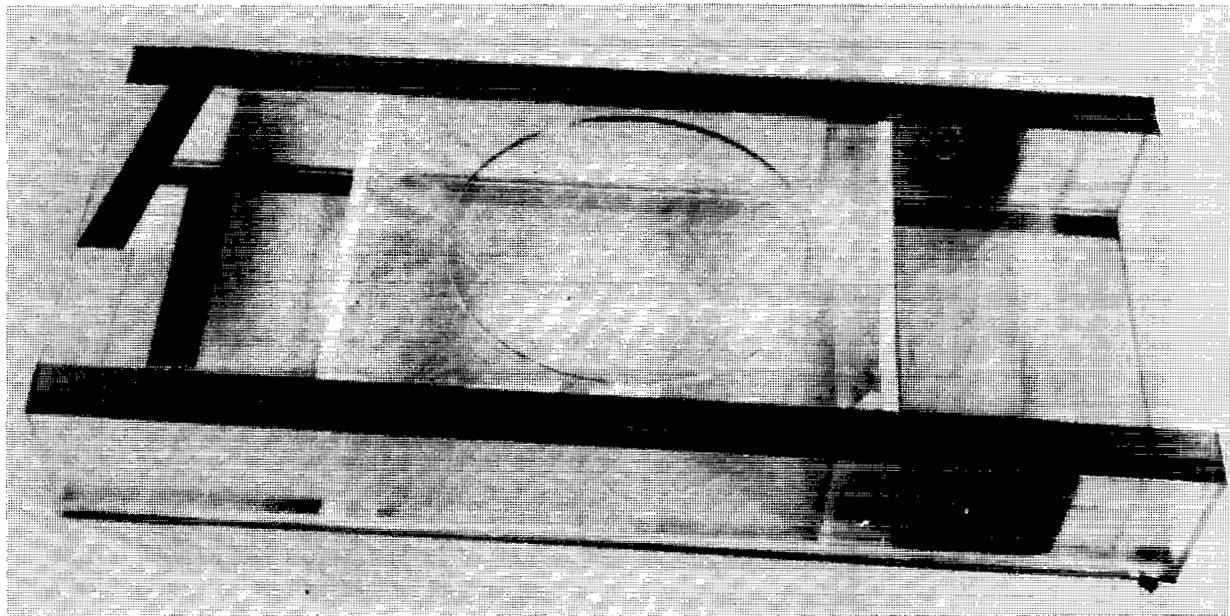
L-69-7549

Figure 7.- Rectangular glass plasma-containing tube.
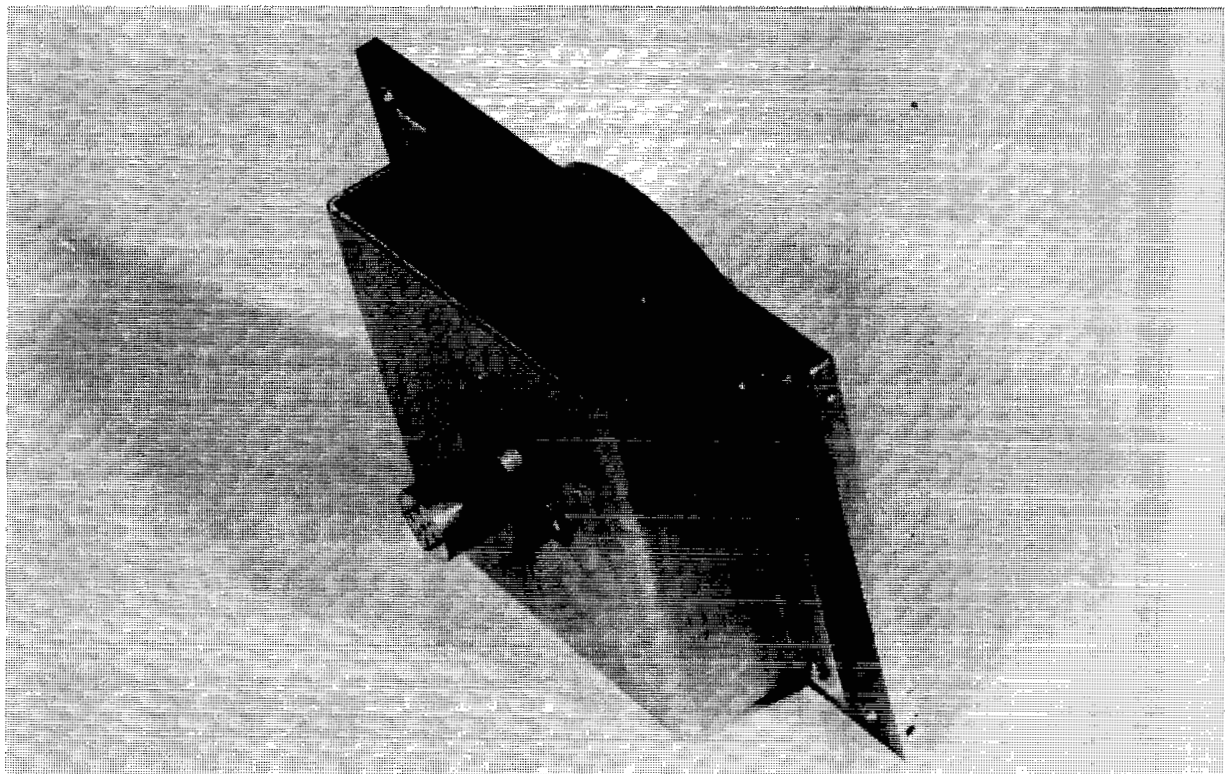
L-69-7684

Figure 8.- E-band horn antenna and mounting bracket with attached reflector plate.
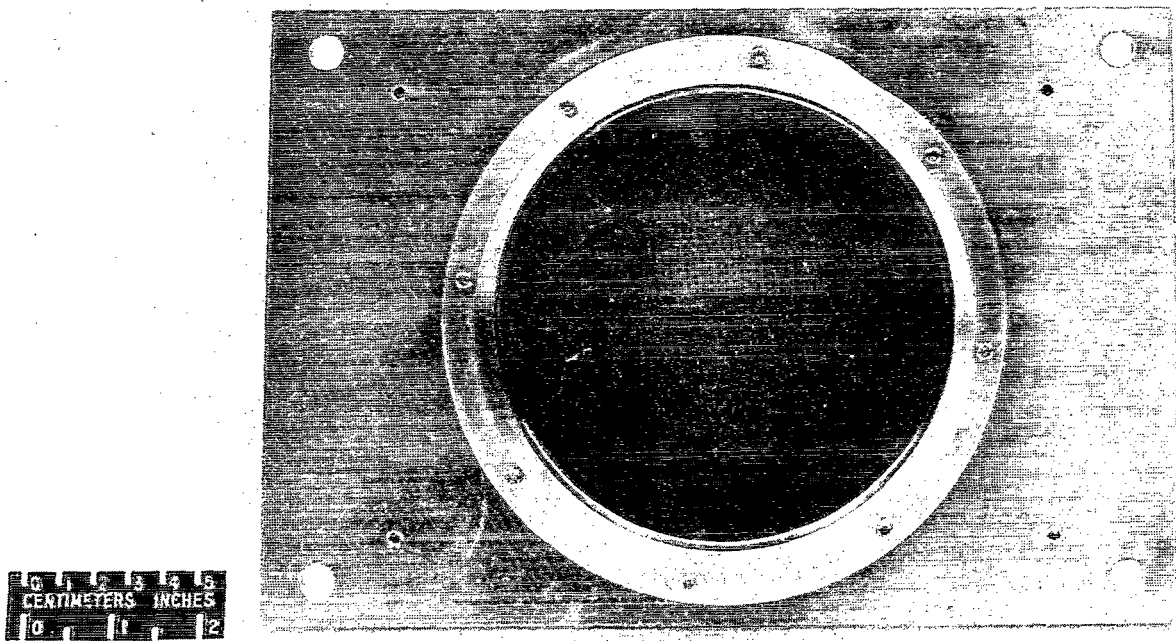
L-69-7687

Figure 9.- Perforated reflector mounted on flat plate.
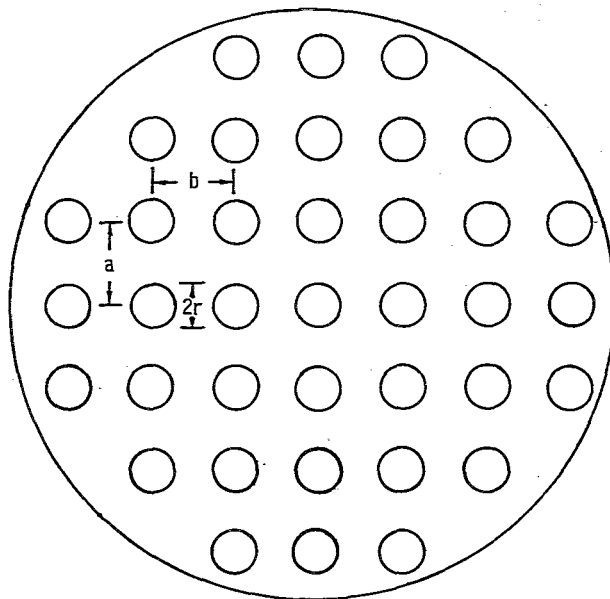
Figure 10.- Hole pattern of reflector plate.
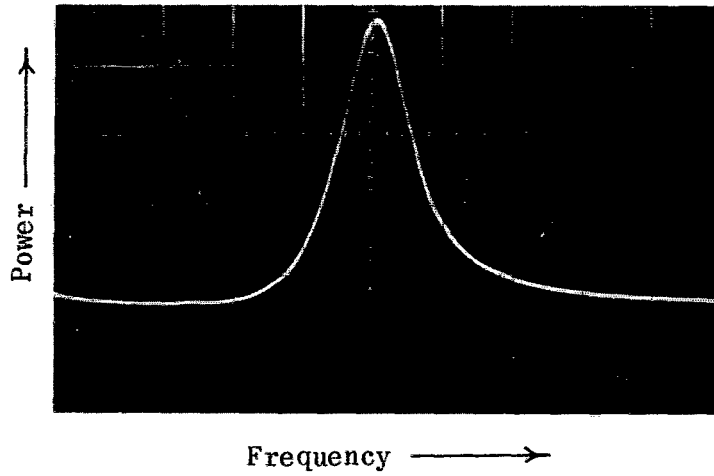
(a)   Cavity response.
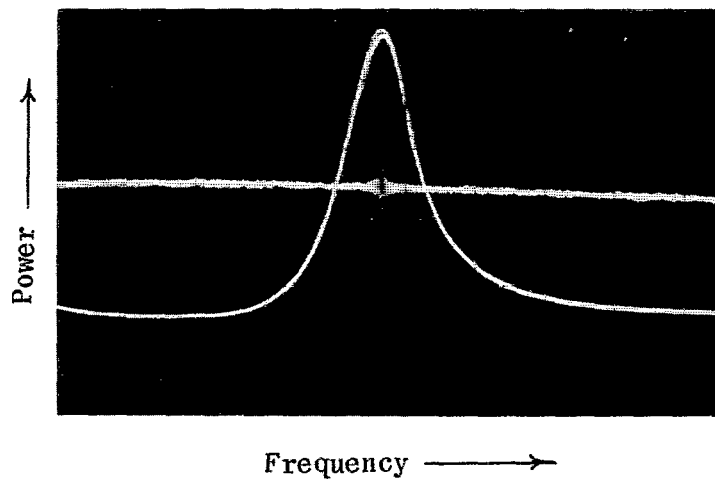
(b)   Cavity response with variable-frequency marker.

Figure 11.- Cavity response curve and variable-frequency marker.
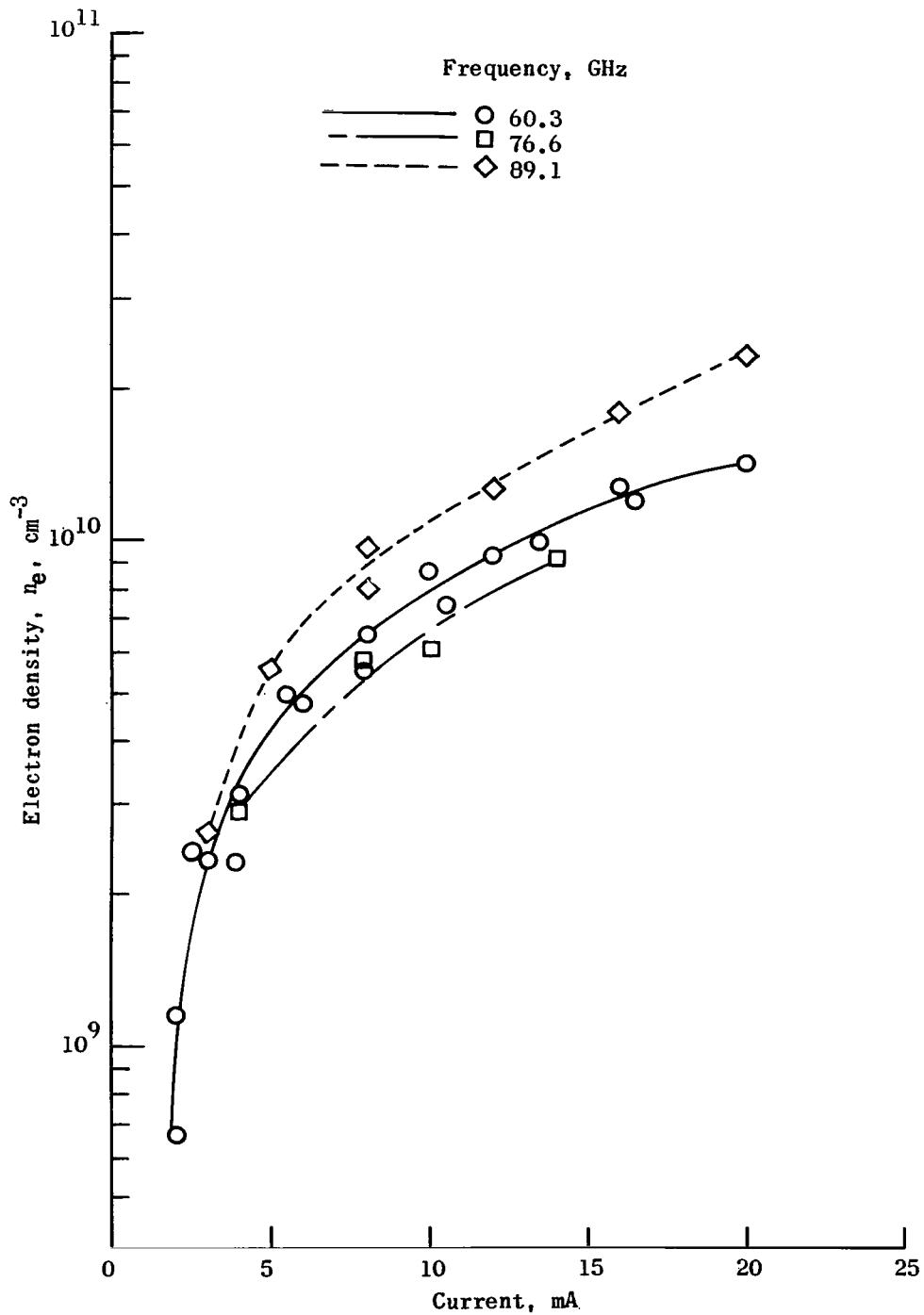
(a) Tube pressure of 0.125 torr.

Figure 12.- Electron density as a function of plasma tube current
for assumed homogeneous plasma.
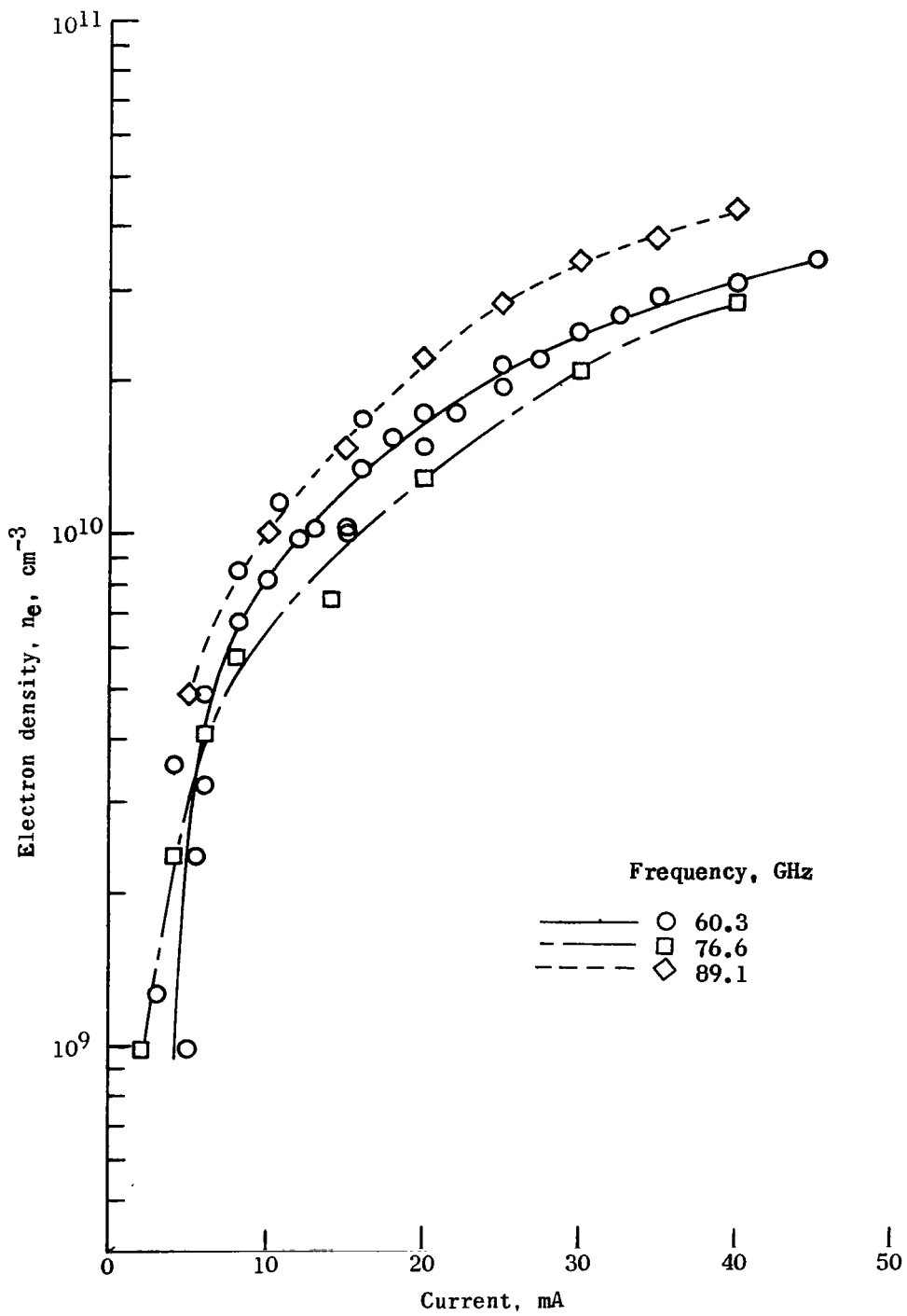
(b) Tube pressure of 0.210 torr.

Figure 12.- Continued.
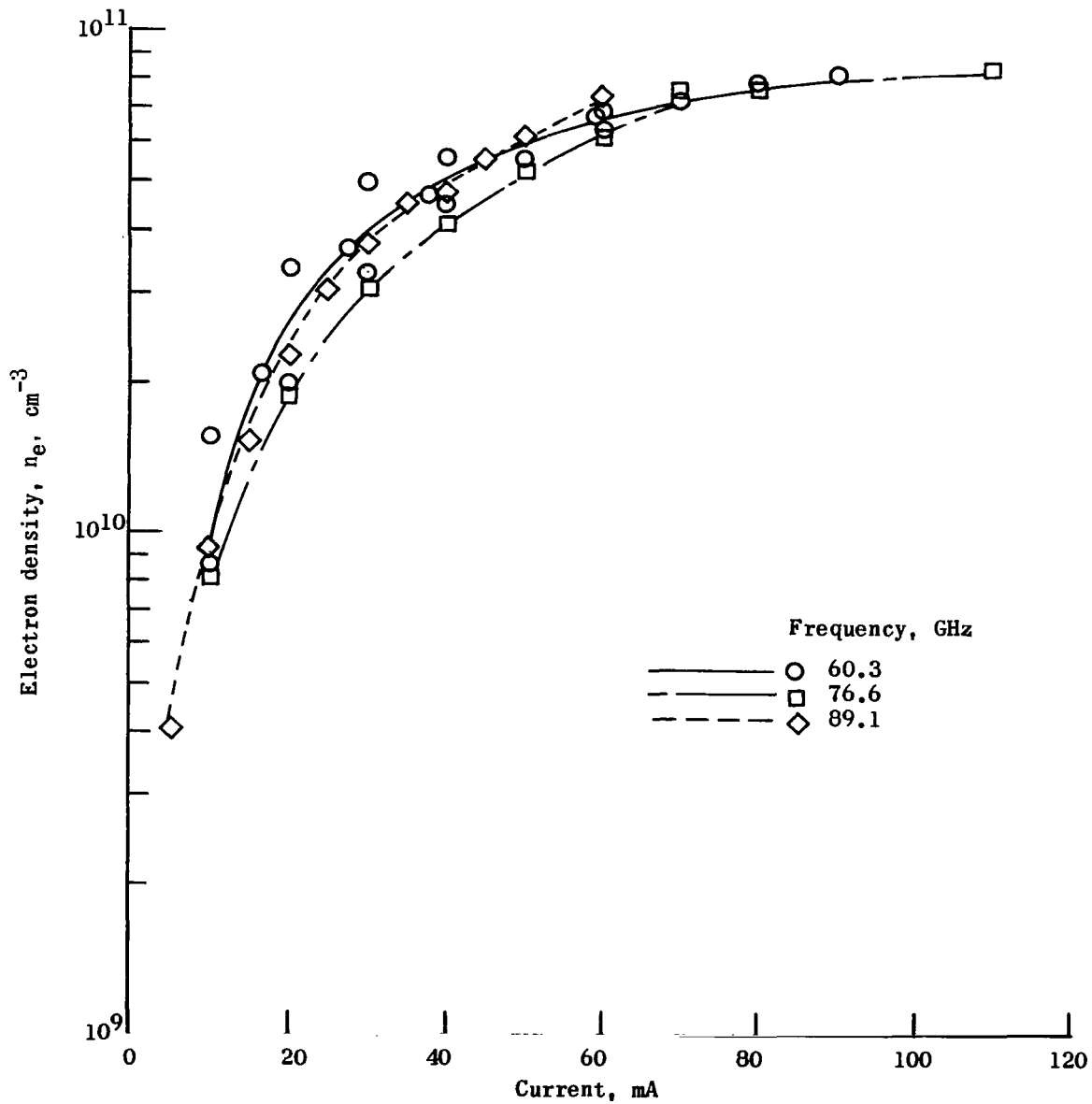
(c) Tube pressure of 0.410 torr.

Figure 12.- Continued.
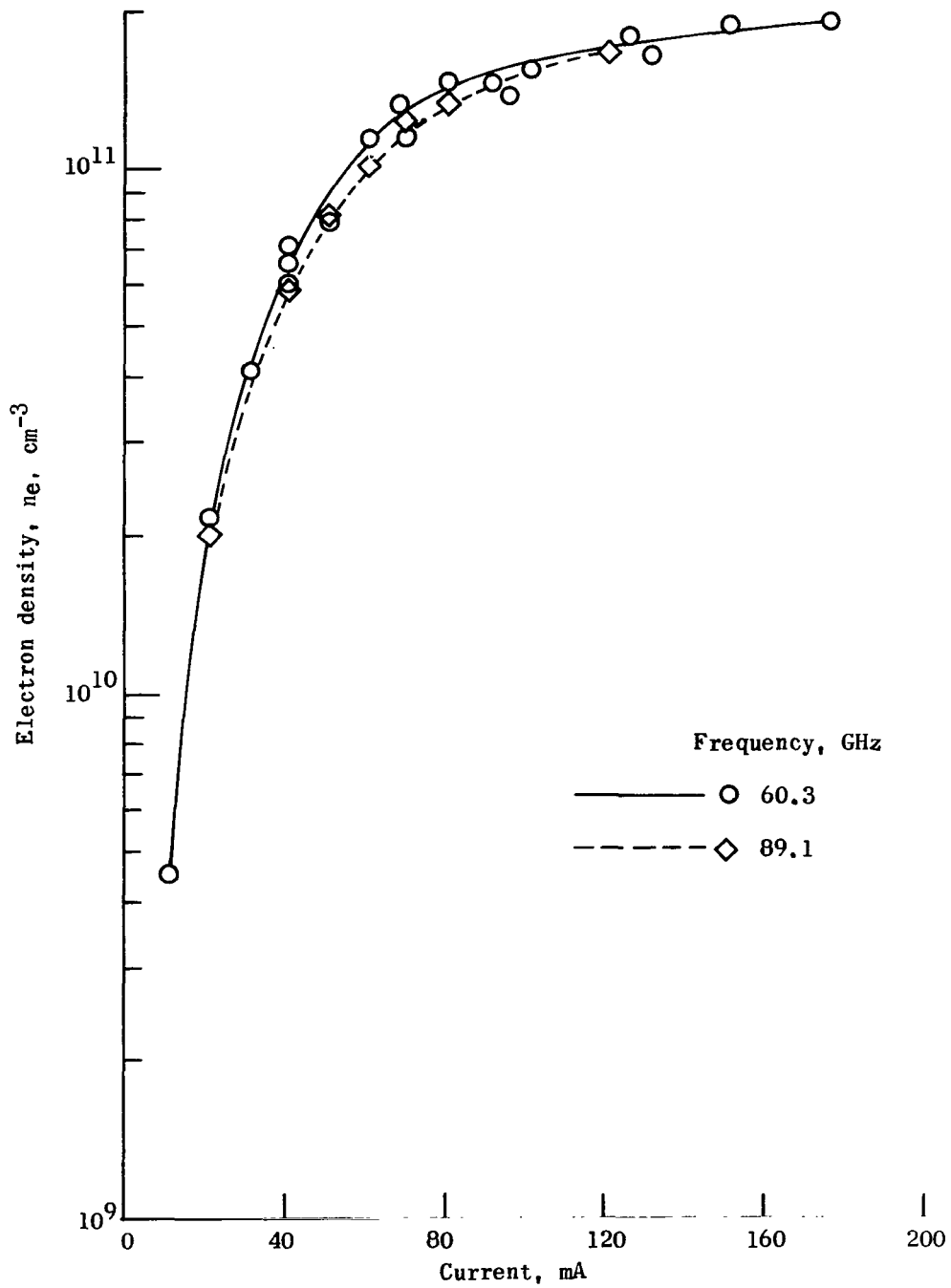
(d) Tube pressure of 0.680 torr.

Figure 12.- Concluded.
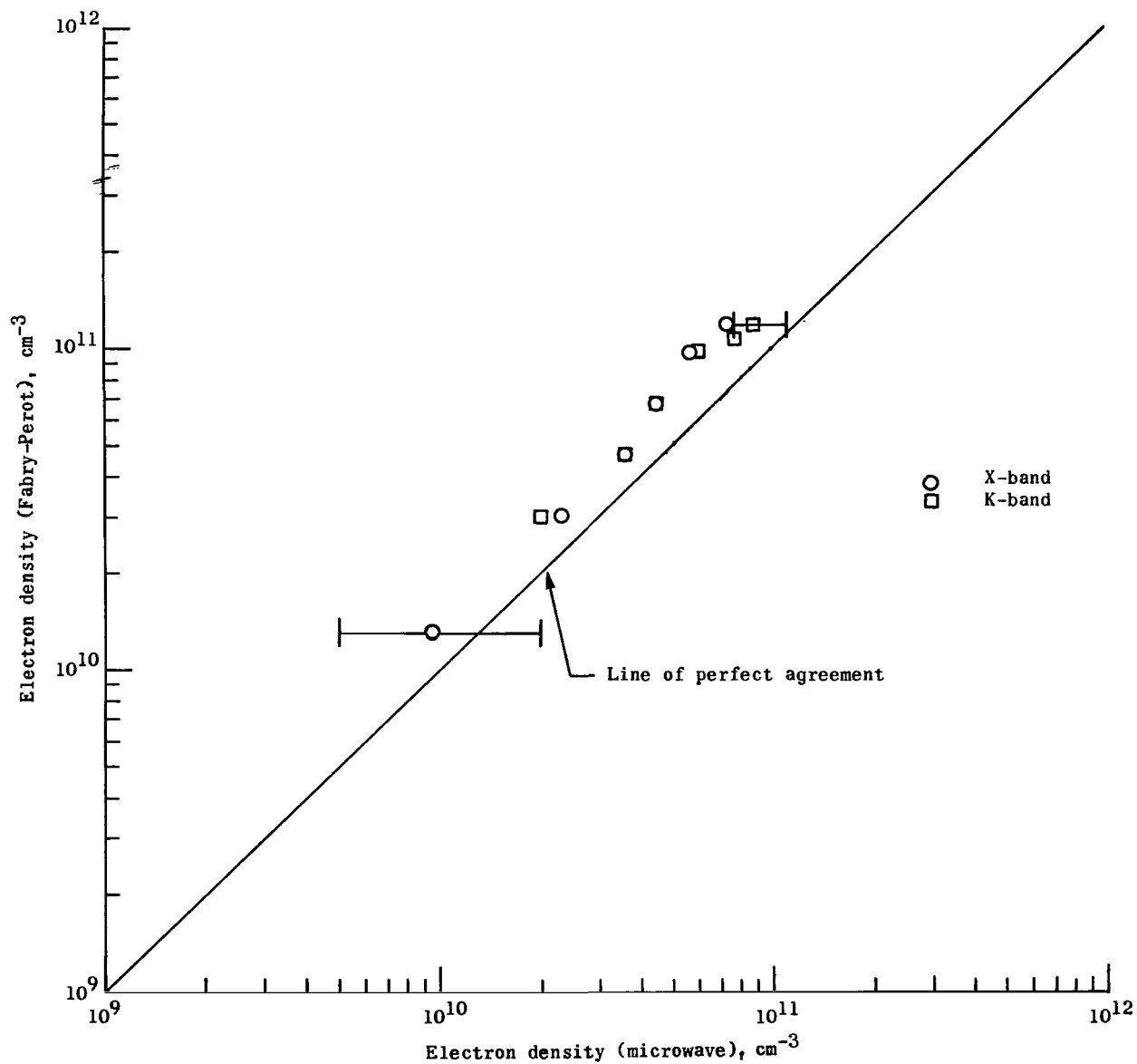
(a) Fabry-Perot frequency of 60.3 GHz.

Figure 13.- Comparison of peak electron density measurements made with Fabry-Perot interferometer and microwave interferometer at tube pressure of 0.410 torr.
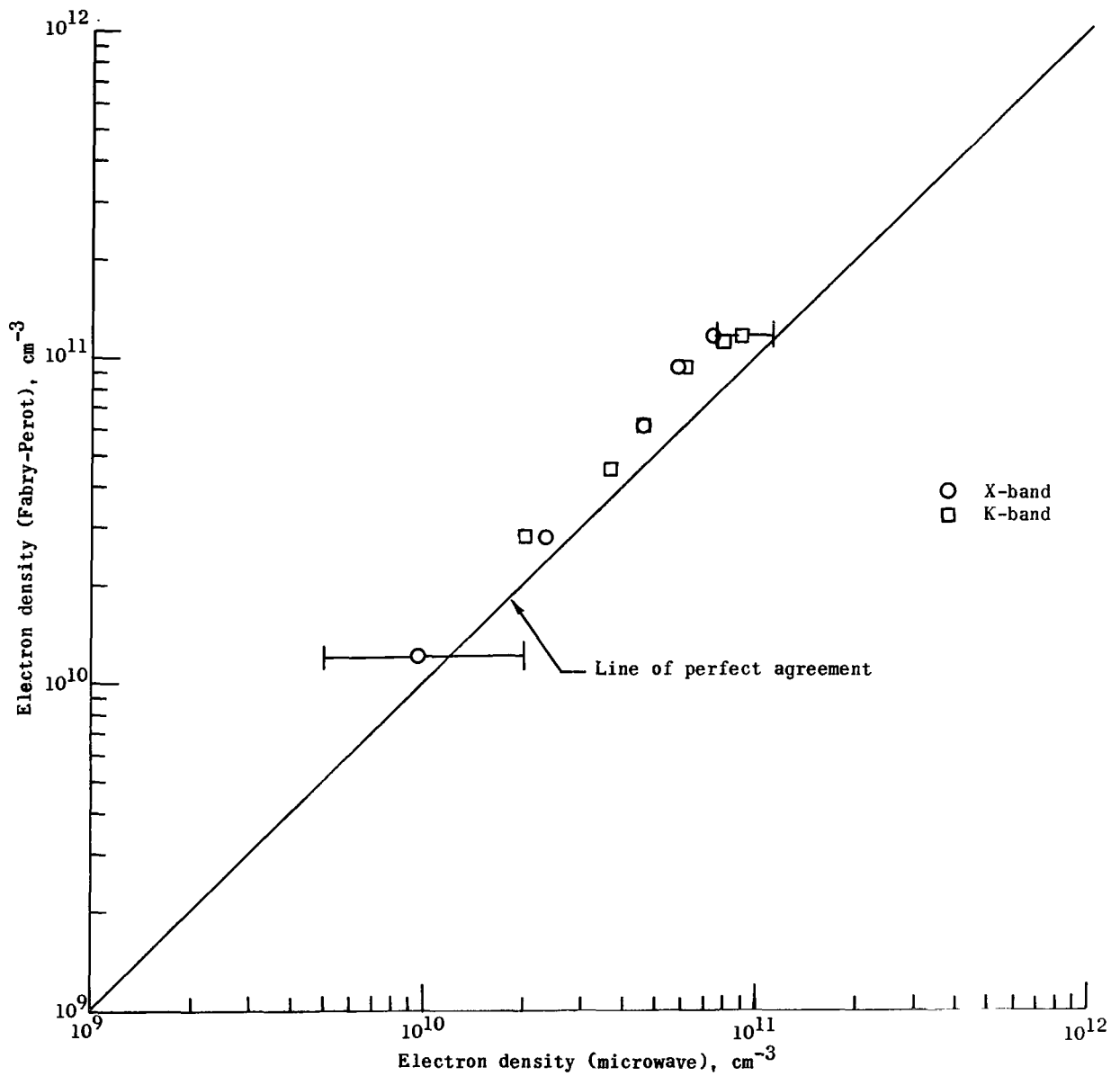
(b) Fabry-Perot frequency of 76.6 GHz.

Figure 13.- Continued.
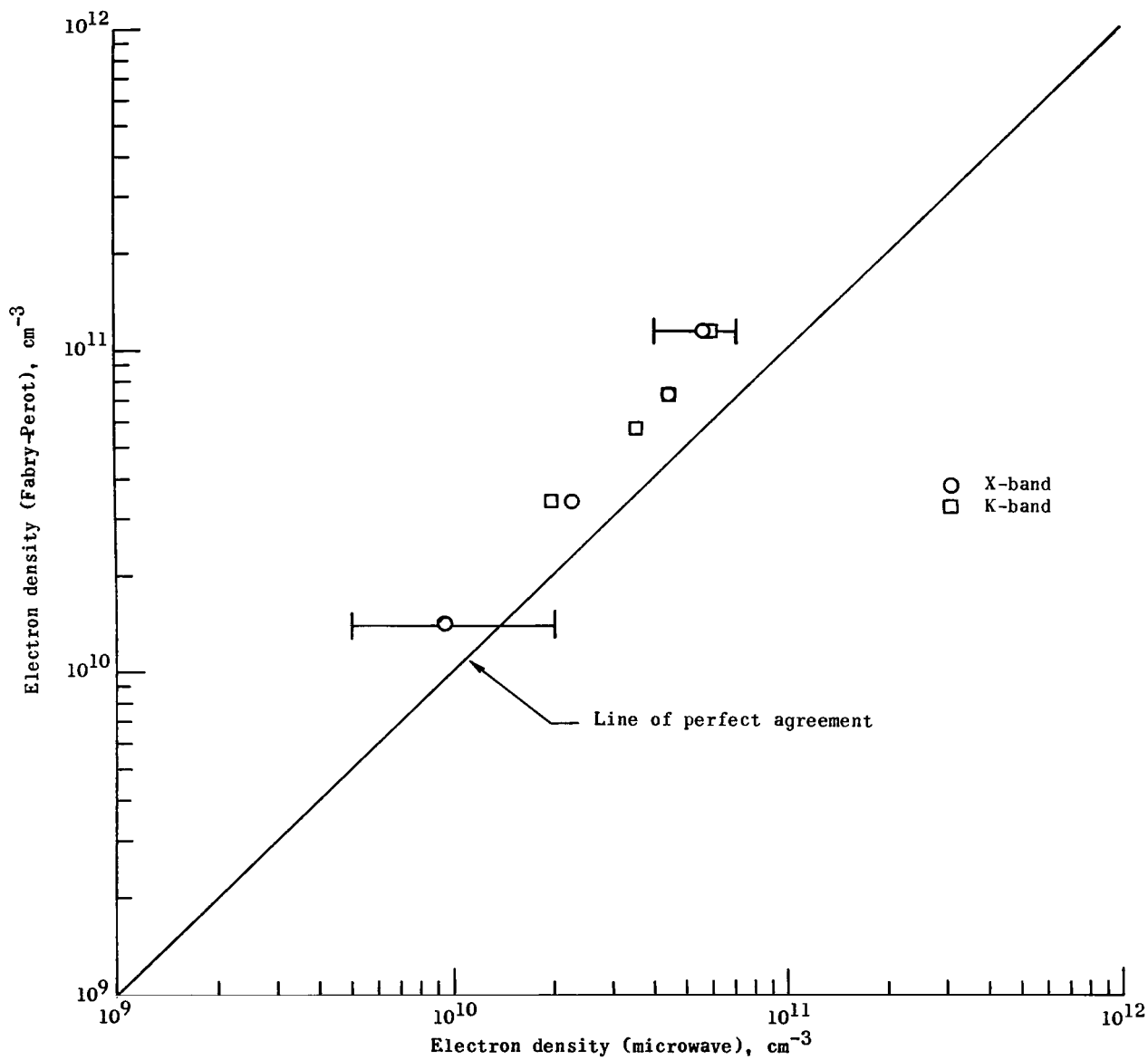
(c) Fabry-Perot frequency of 89.1 GHz.

Figure 13.- Concluded.
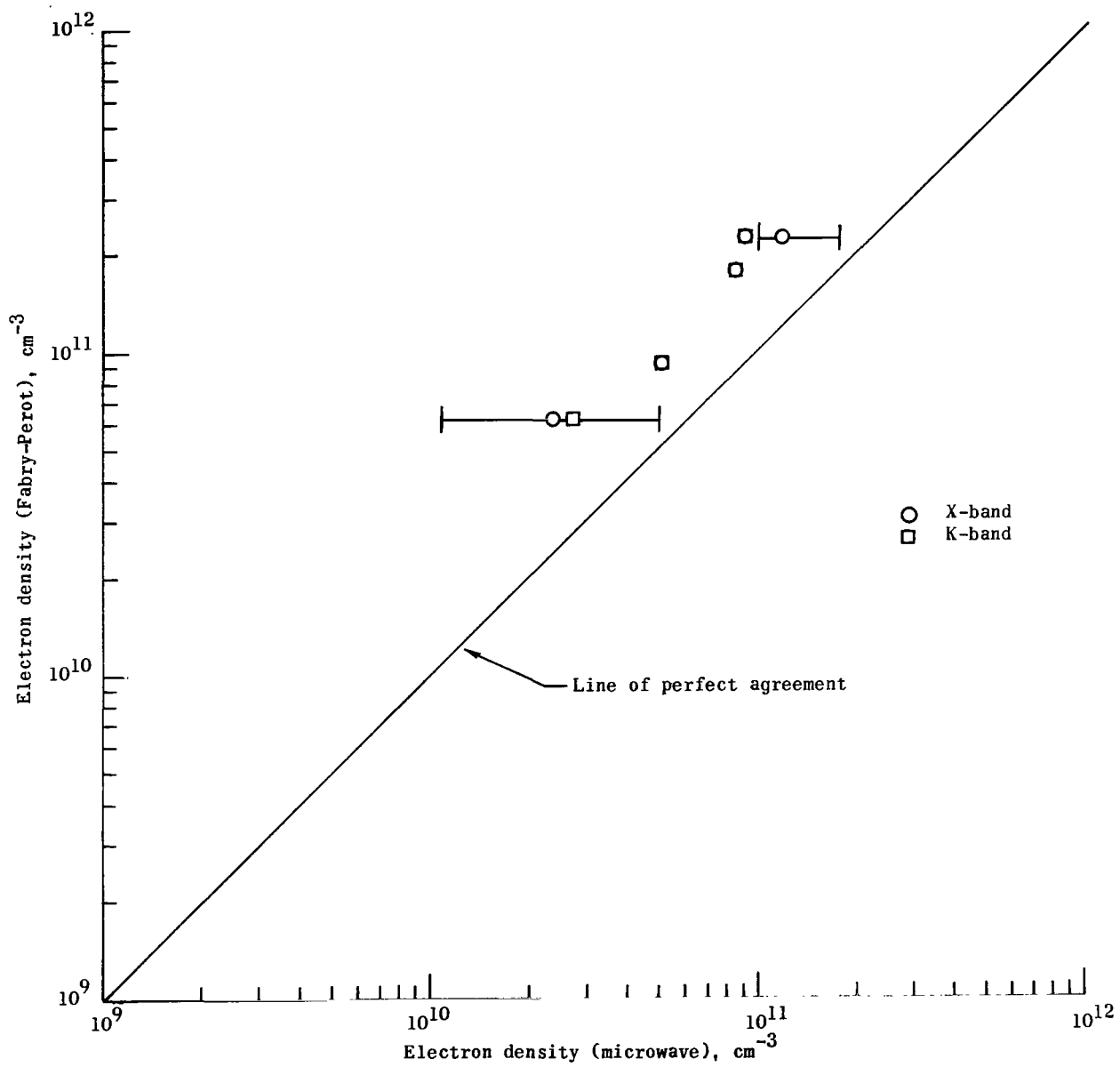
(a) Fabry-Perot frequency of 60.3 GHz.

Figure 14.- Comparison of peak electron density measurements made with Fabry-Perot interferometer and microwave interferometer at tube pressure of 0.680 torr.
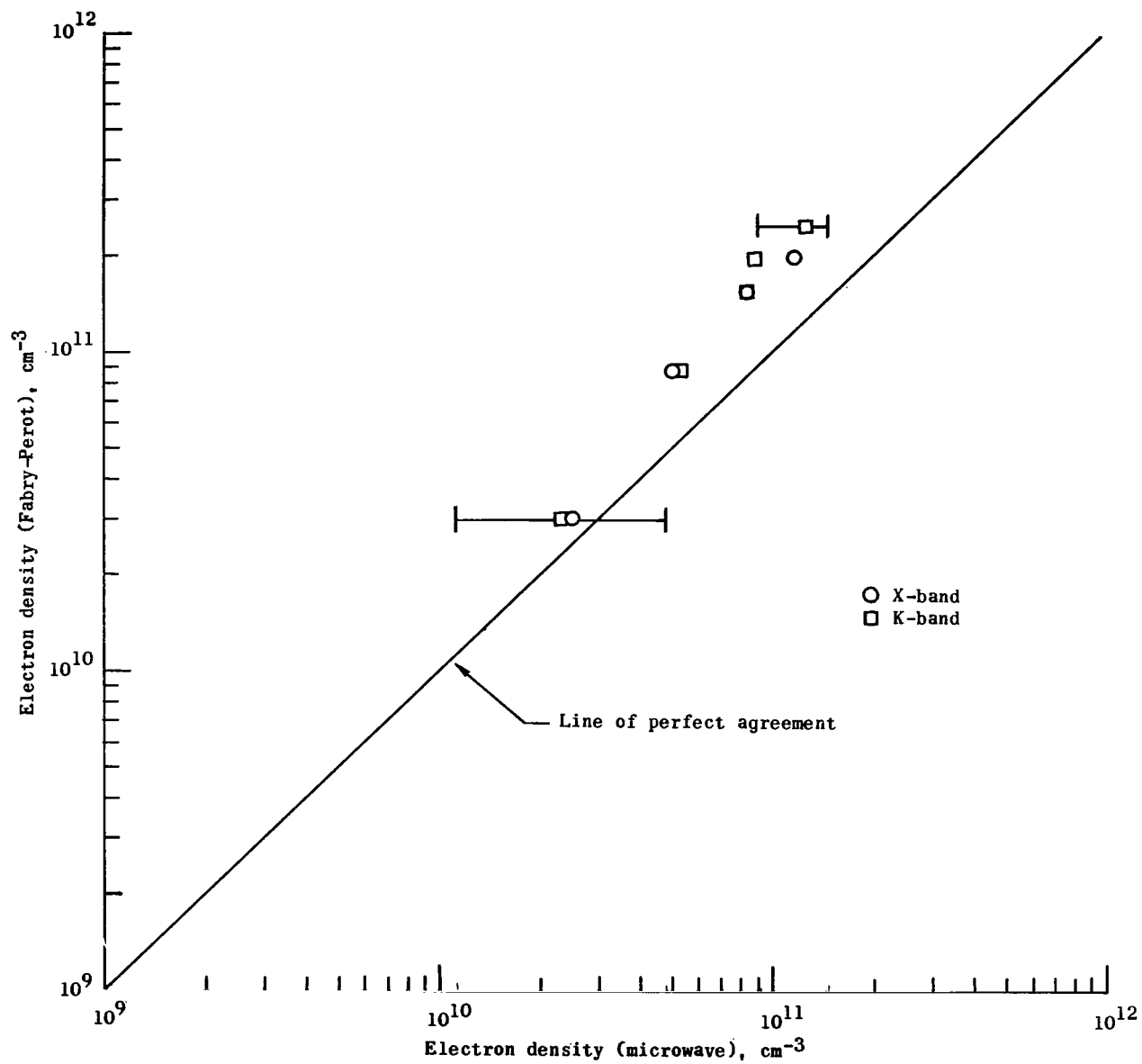
(b) Fabry-Perot frequency of 89.1 GHz.

Figure 14.- Concluded.

"The aeronautical and space activities of the United States shall be conducted so as to contribute . . . to the expansion of human knowledge of phenomena in the atmosphere and space. The Administration shall provide for the widest practicable and appropriate dissemination of information concerning its activities and the results thereof."

— NATIONAL AERONAUTICS AND SPACE ACT OF 1958

NASA SCIENTIFIC AND TECHNICAL PUBLICATIONS

TECHNICAL REPORTS: Scientific and technical information considered important, complete, and a lasting contribution to existing knowledge.

TECHNICAL NOTES: Information less broad in scope but nevertheless of importance as a contribution to existing knowledge.

TECHNICAL MEMORANDUMS: Information receiving limited distribution because of preliminary data, security classification, or other reasons.

CONTRACTOR REPORTS: Scientific and technical information generated under a NASA contract or grant and considered an important contribution to existing knowledge.

TECHNICAL TRANSLATIONS: Information published in a foreign language considered to merit NASA distribution in English.

SPECIAL PUBLICATIONS: Information derived from or of value to NASA activities. Publications include conference proceedings, monographs, data compilations, handbooks, sourcebooks, and special bibliographies.

TECHNOLOGY UTILIZATION PUBLICATIONS: Information on technology used by NASA that may be of particular interest in commercial and other non-aerospace applications. Publications include Tech Briefs, Technology Utilization Reports and Technology Surveys.

Details on the availability of these publications may be obtained from:

SCIENTIFIC AND TECHNICAL INFORMATION OFFICE

NATIONAL AERONAUTICS AND SPACE ADMINISTRATION
Washington, D.C. 20546